Synthesis Of Tetraphosphine Macrocycles Using Copper(I) Templates

Bryan P. Nell, Charles D. Swor, E. Adrian Henle, Lev N. Zakharov, N. Ian Rinehart,

*Aditya Nathan, and David R. Tyler**

Department of Chemistry and Biochemistry, University of Oregon, Eugene, OR, 97403,

USA

E-mail: dtyler@uoregon.edu

Table of Contents

Table S1. Mass spectral data for copper macrocyclic complexes **12-17**.

complex	R	n	m	Formula	*m/z*[a]
12	$CH_3O(C_3H_6)$	1	1	$[C_{26}H_{56}O_4P_4Cu]^+$	619
13	$CH_3O(C_3H_6)$	2	1	$[C_{28}H_{60}O_4P_4Cu]^+$	647
14	Ph	1	1	$[C_{34}H_{40}P_4Cu]^+$	635
15	Ph	2	1	$[C_{36}H_{44}P_4Cu]^+$	663
16	Ph	1	2	$[C_{36}H_{44}P_4Cu]^+$	663
17	Ph	2	2	$[C_{38}H_{48}P_4Cu]^+$	691

[a]calculated and observed

Demetallation of Complex 16. Complex **16** was demetallated with KCN to give the free phosphine **23** as an oily, colorless residue (Scheme 13). The uncoordinated macrocycle ligand displayed a singlet in the $^{31}P\{^1H\}$ NMR spectra at -20.4 ppm. The general features of the ^1H NMR spectrum are broad and do not give much structural information, but the disappearance of the P-H protons support the idea that full alkylation was achieved. A FAB mass spectrum of **19** showed the expected molecular ion peak plus a proton at 601 m/z, and high resolution mass spectrometry (HR-MS) gave a molecular formula of $C_{36}H_{45}P_4$, which corresponds to $[m+H]^+$.

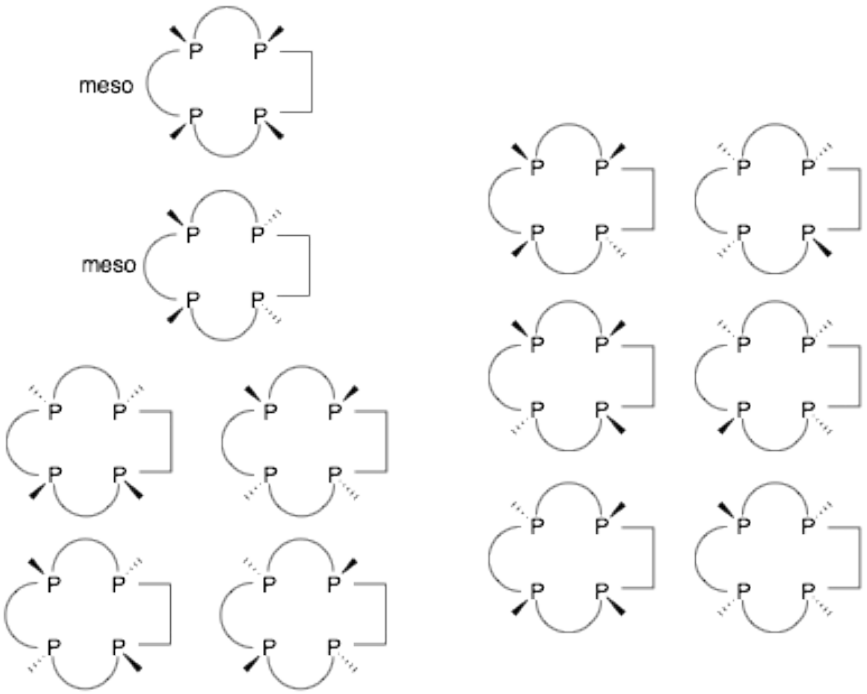

Figure S1. Possible stereoisomers of phosphine **21** (arc = -C_3H_6-, box = -C_4H_8-).

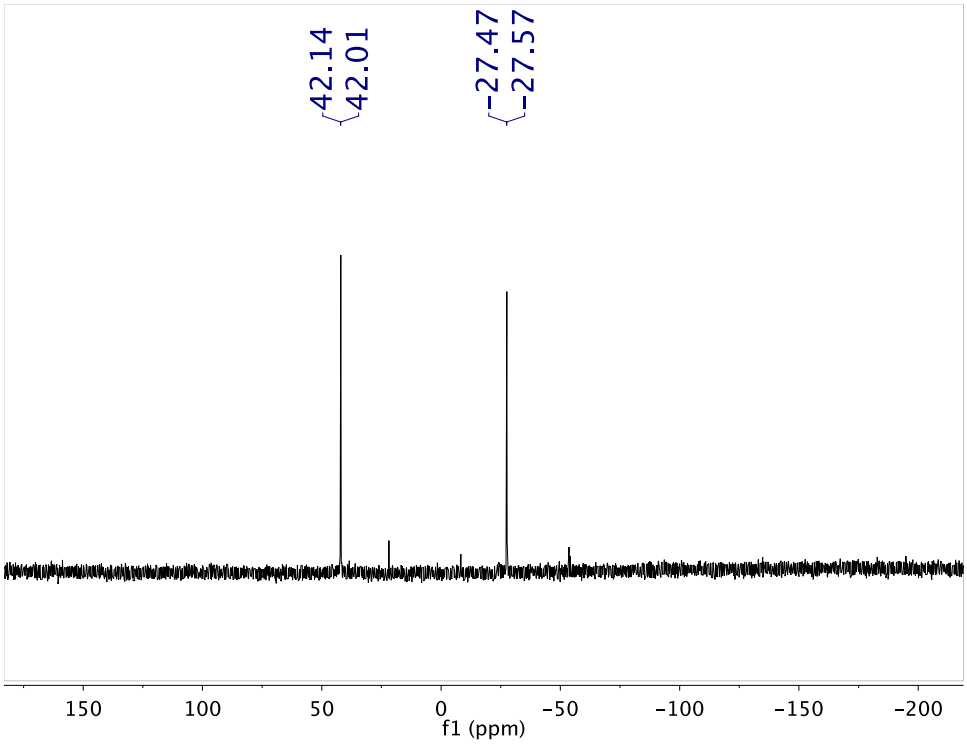

Figure S2. $^{31}P\{^1H\}$ NMR spectrum of **3** in $CDCl_3$.

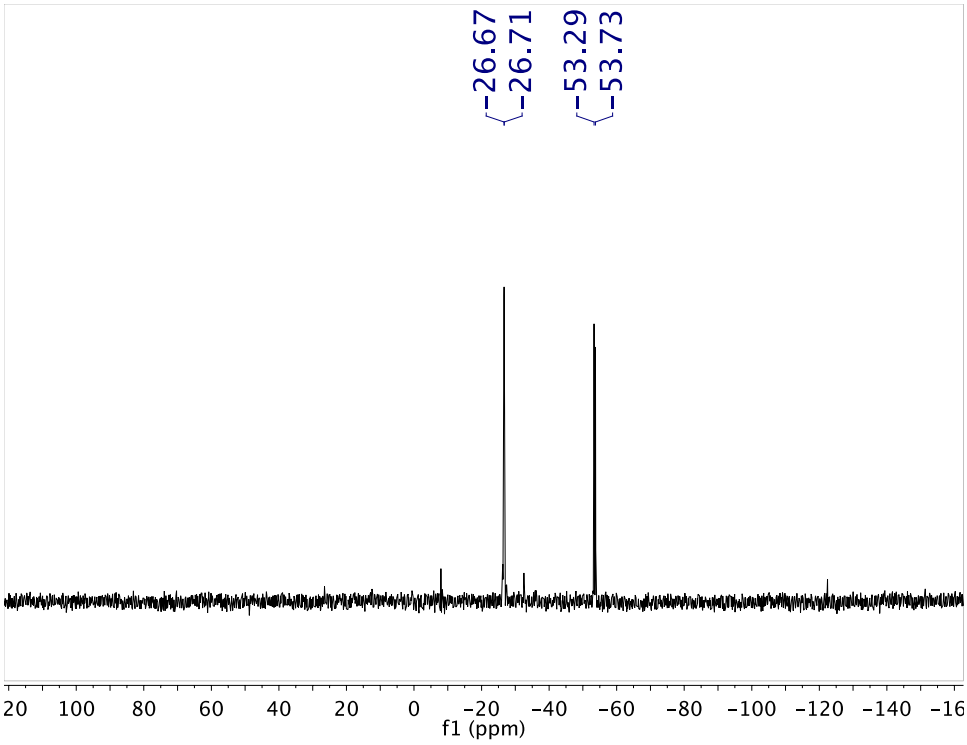

Figure S3. $^{31}P\{^{1}H\}$ NMR spectrum of **4** in $CDCl_3$.

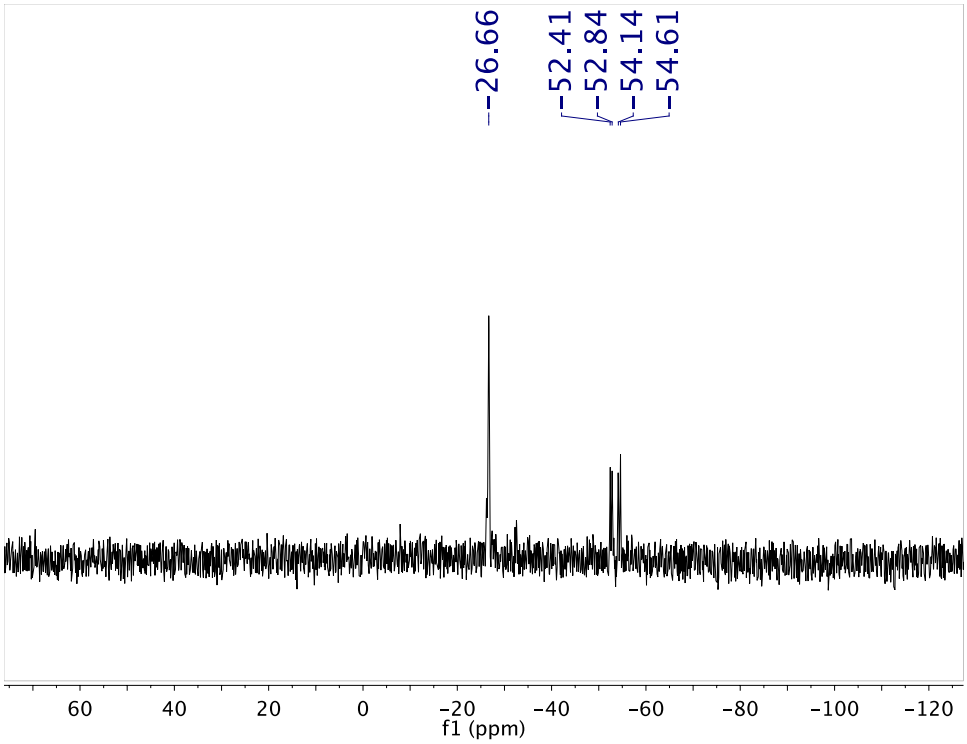

Figure S4. ^{31}P NMR spectrum of **4** in $CDCl_3$.

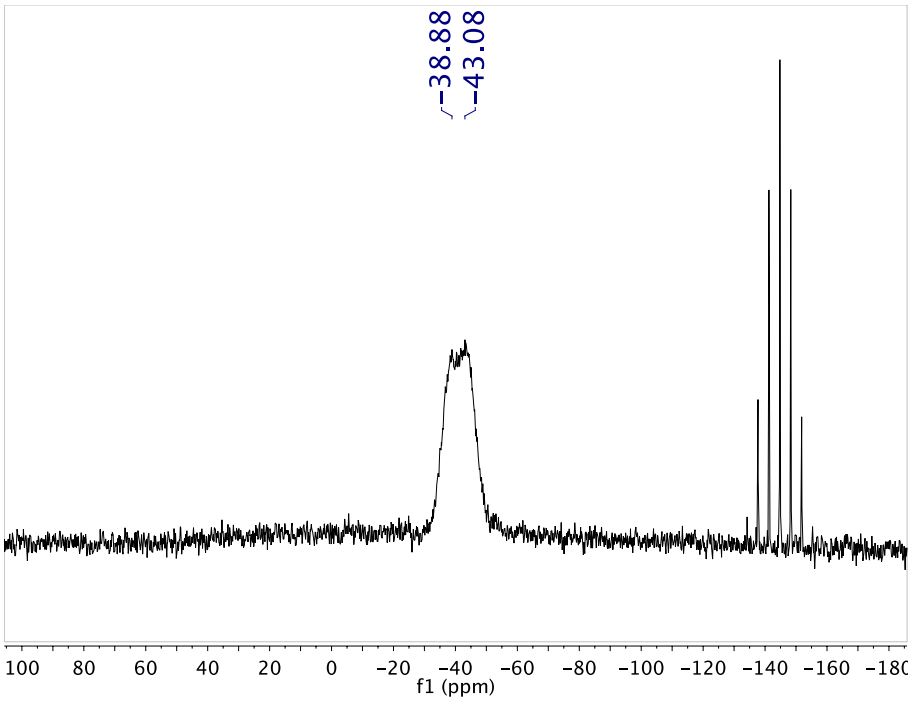

Figure S5. $^{31}P\{^{1}H\}$ NMR spectrum of $Cu(MeOPrPE)_2PF_6$ (**7**) in $CDCl_3$.

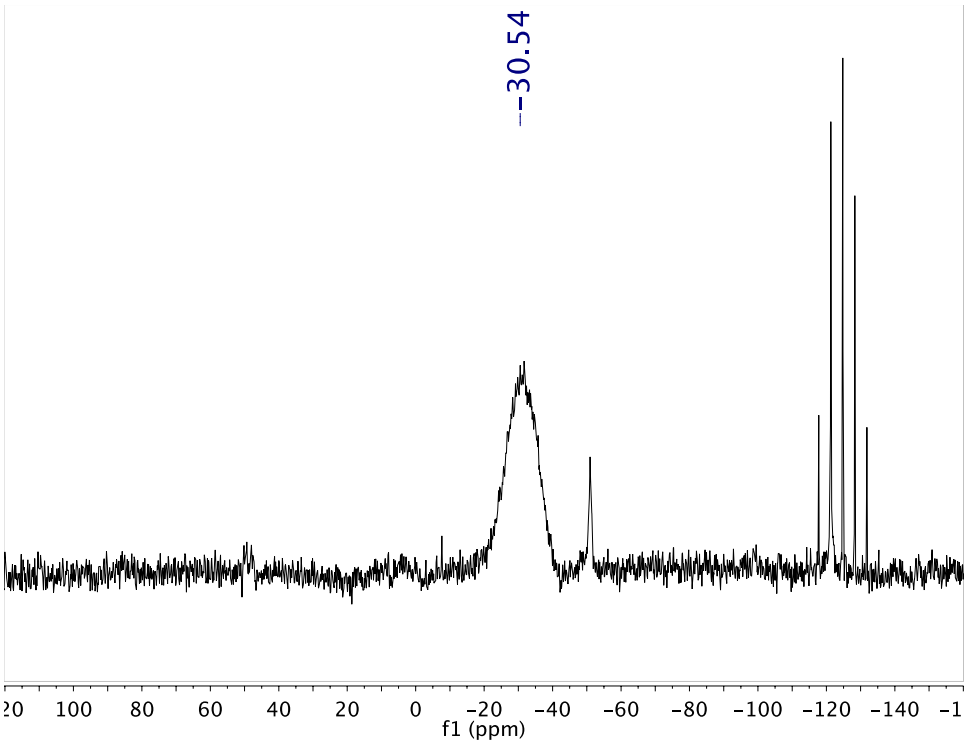

Figure S6. $^{31}P\{^{1}H\}$ NMR spectrum of $Cu(MeOPrPP)_2PF_6$ (**8**) in $CDCl_3$. Note this spectrum is for the PF_6^- salt. The PF_6^- resonance is at approximately -125 ppm.

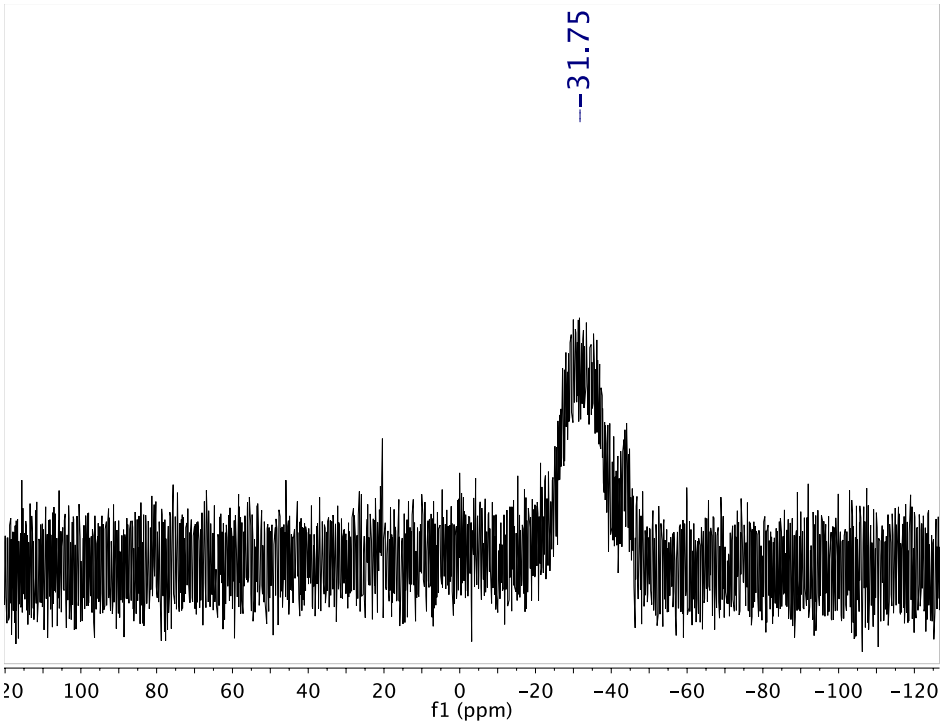

Figure S7. $^{31}P\{^{1}H\}$ NMR spectrum of $Cu(MPPE)_2OTf$ (**9**) in $CDCl_3$.

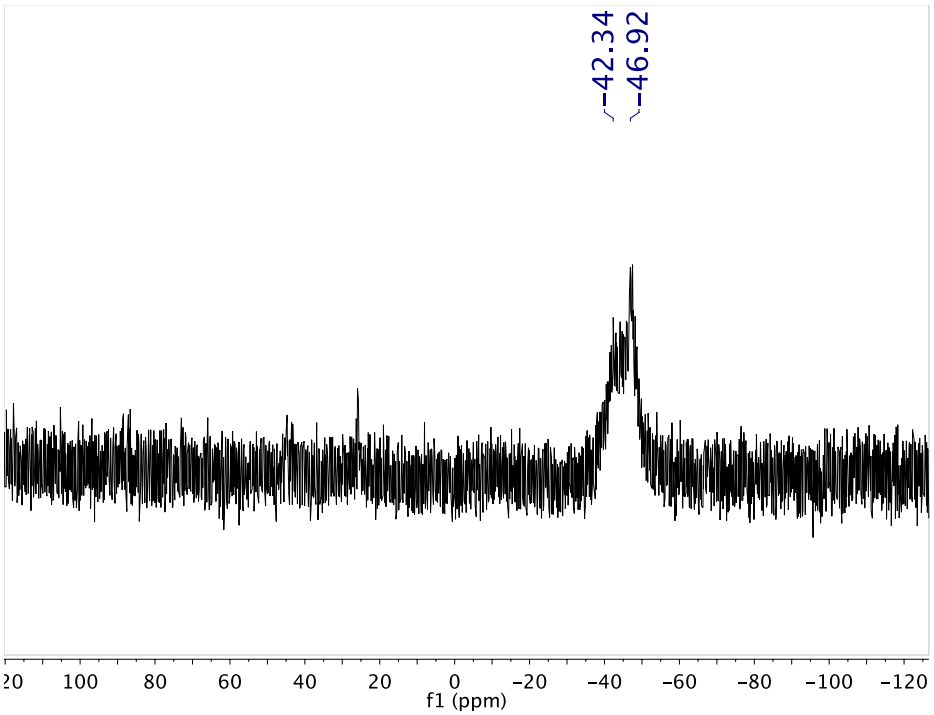

Figure S8. $^{31}P\{^{1}H\}$ NMR spectrum of $Cu(MPPP)_2OTf$ (**10**) in $CDCl_3$.

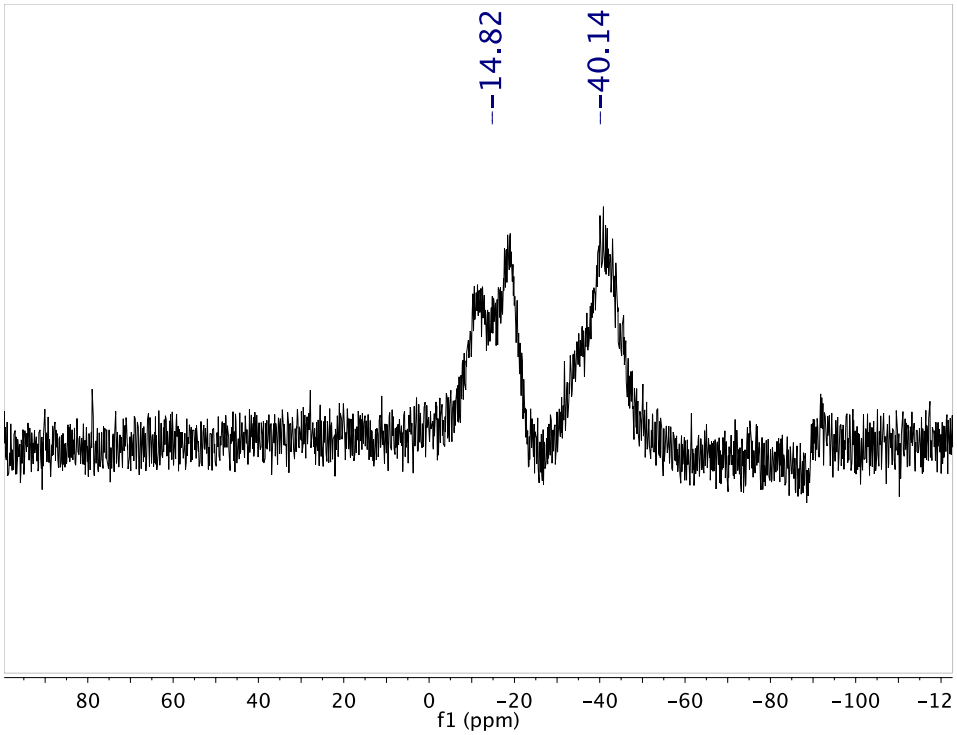

Figure S9. $^{31}P\{^{1}H\}$ NMR spectrum of **11** in $CDCl_3$.

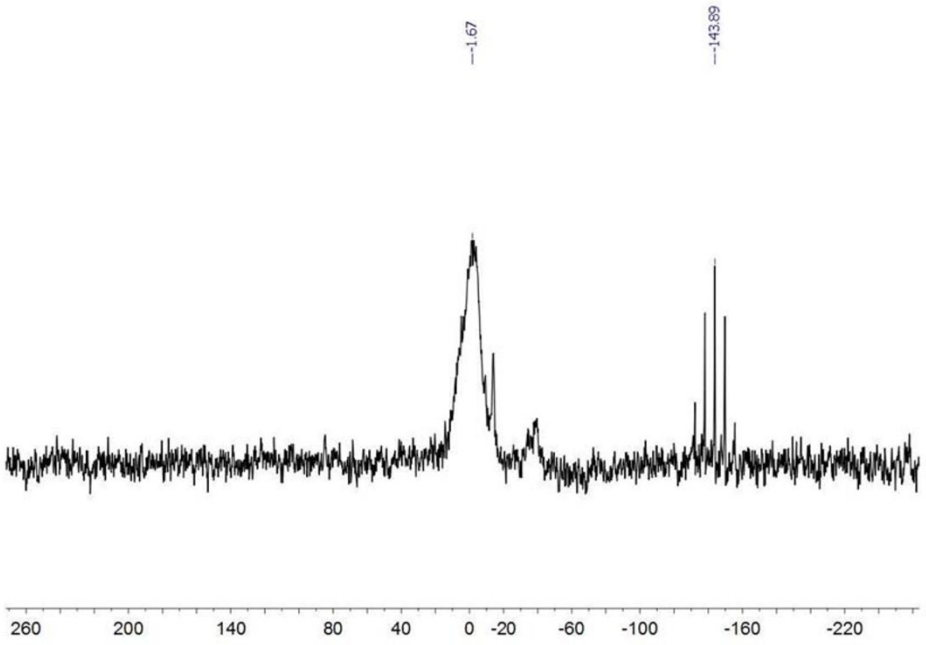

Figure S10. $^{31}P\{^{1}H\}$ NMR spectrum of **12** in $CDCl_3$.

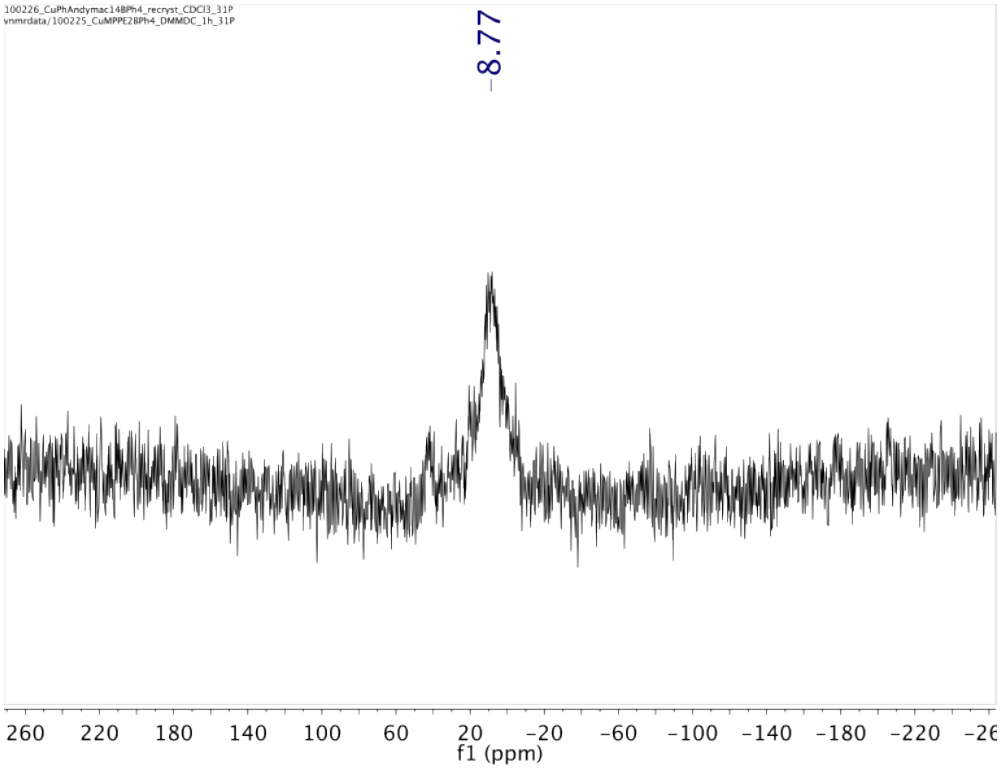

Figure S11. $^{31}P\{^{1}H\}$ NMR spectrum of **14** in $CDCl_3$.

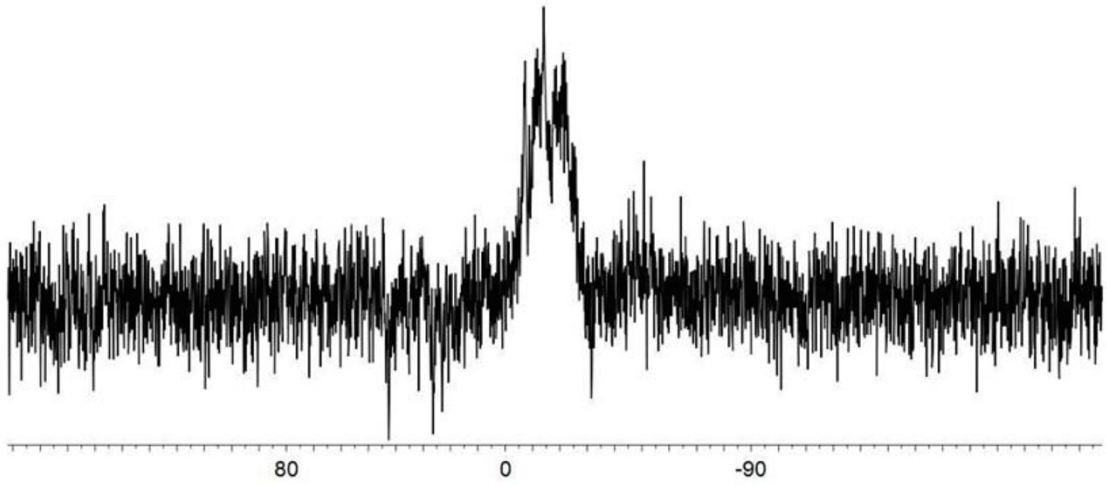

Figure S12. $^{31}P\{^{1}H\}$ NMR spectrum of **15** in $CDCl_3$.

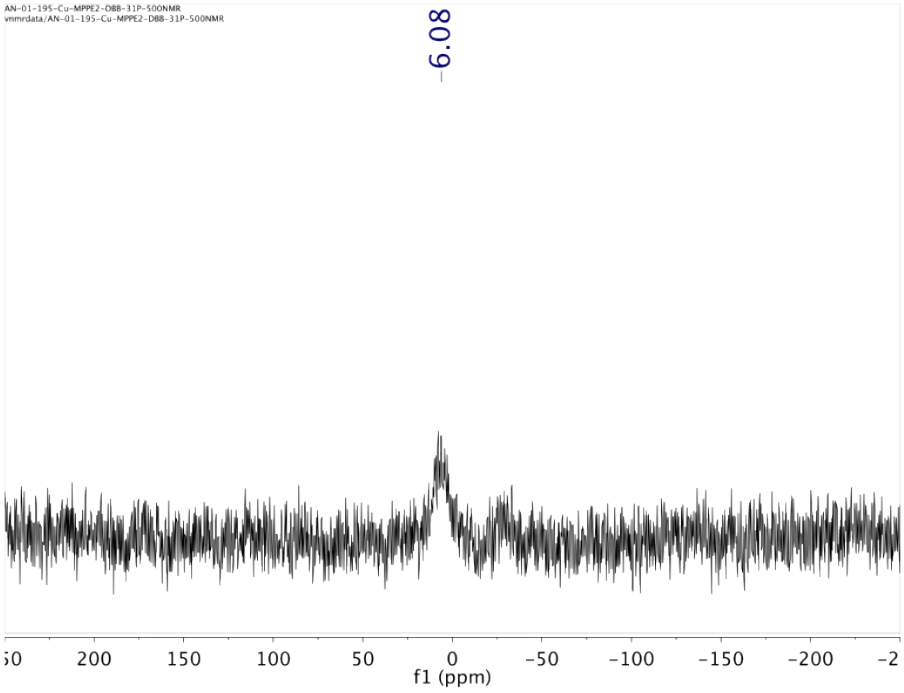

Figure S13. $^{31}P\{^{1}H\}$ NMR spectrum of **16** in $CDCl_3$.

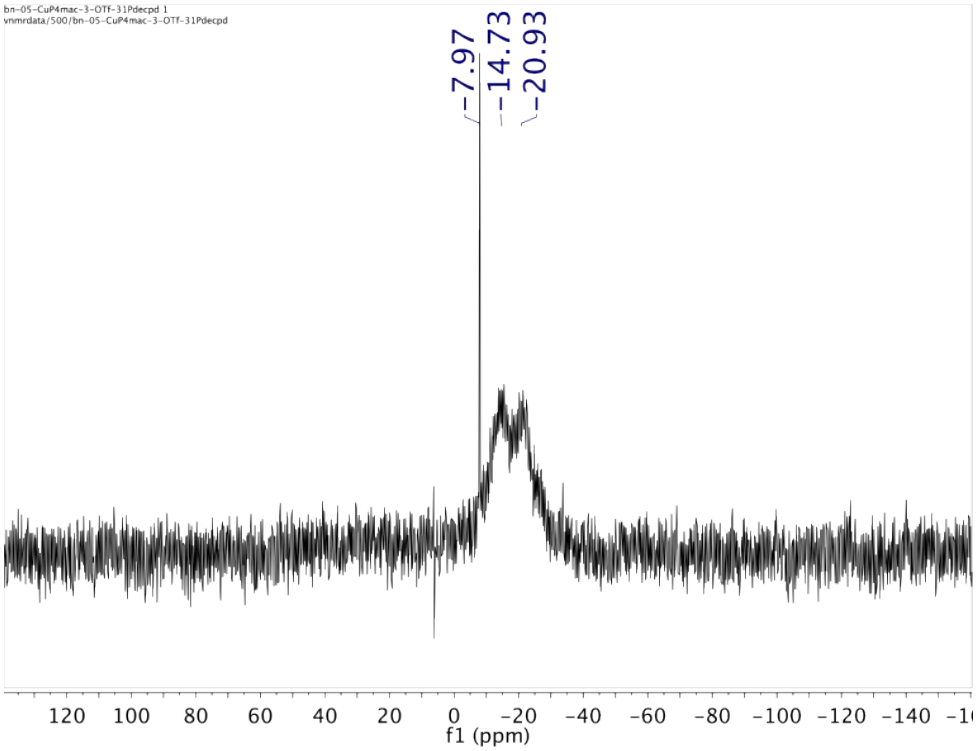

Figure S14. $^{31}P\{^{1}H\}$ NMR spectrum of **15** from **11**.

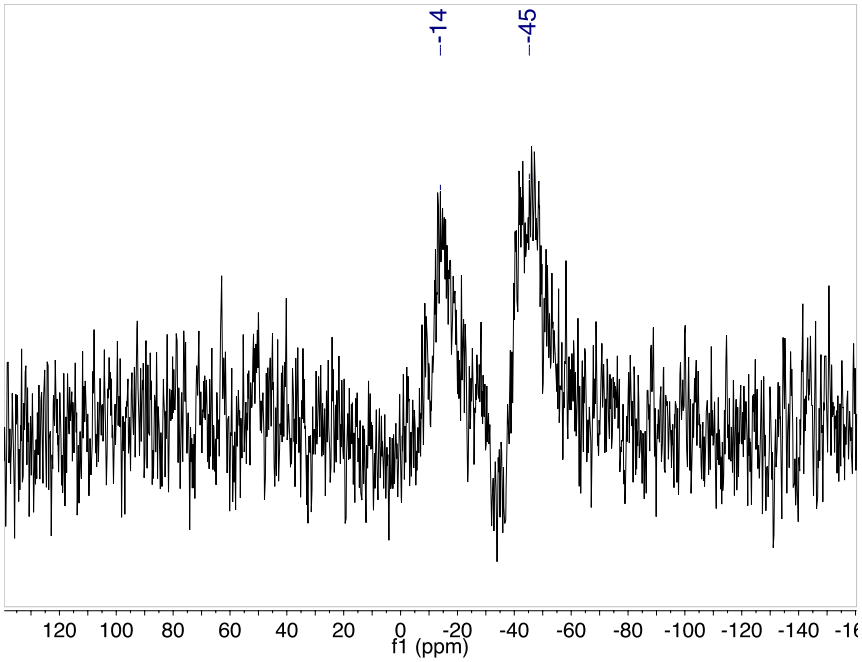

Figure S15. $^{31}P\{^{1}H\}$ NMR spectrum of **17**.

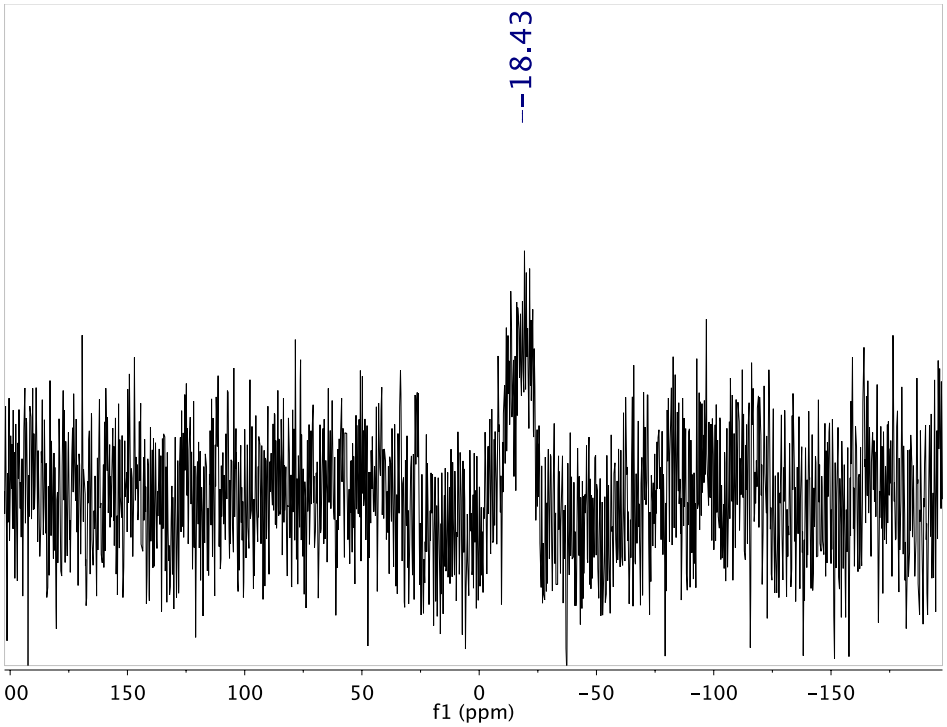

Figure S16. $^{31}P\{^{1}H\}$ NMR spectrum of **18** in $CDCl_3$.

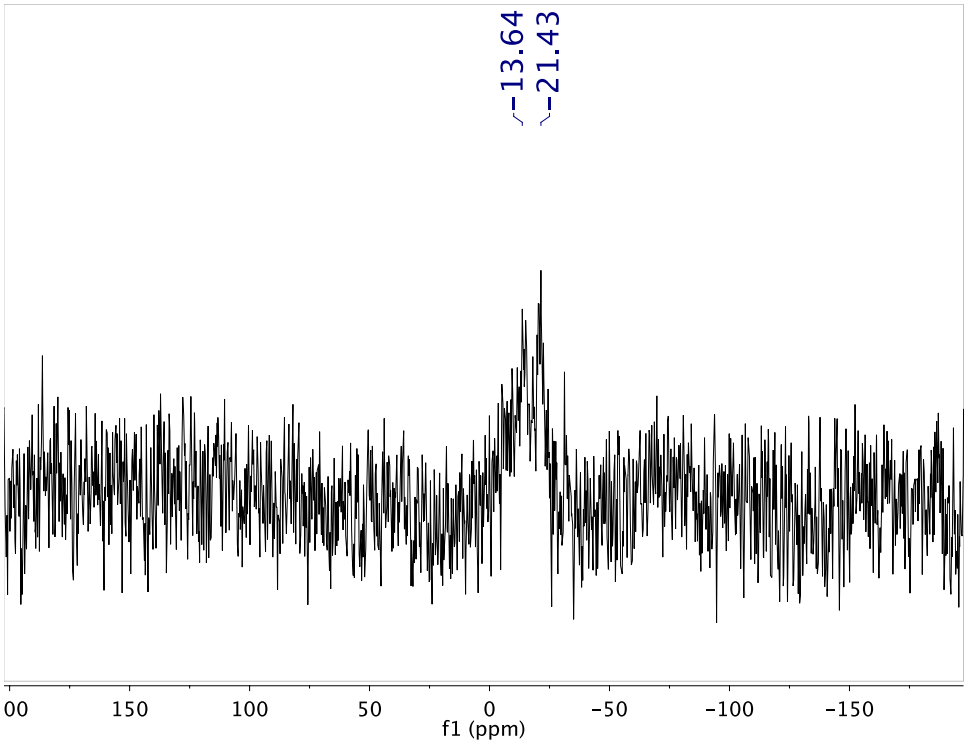

Figure S17. $^{31}P\{^{1}H\}$ NMR spectrum of **19** in $CDCl_3$.

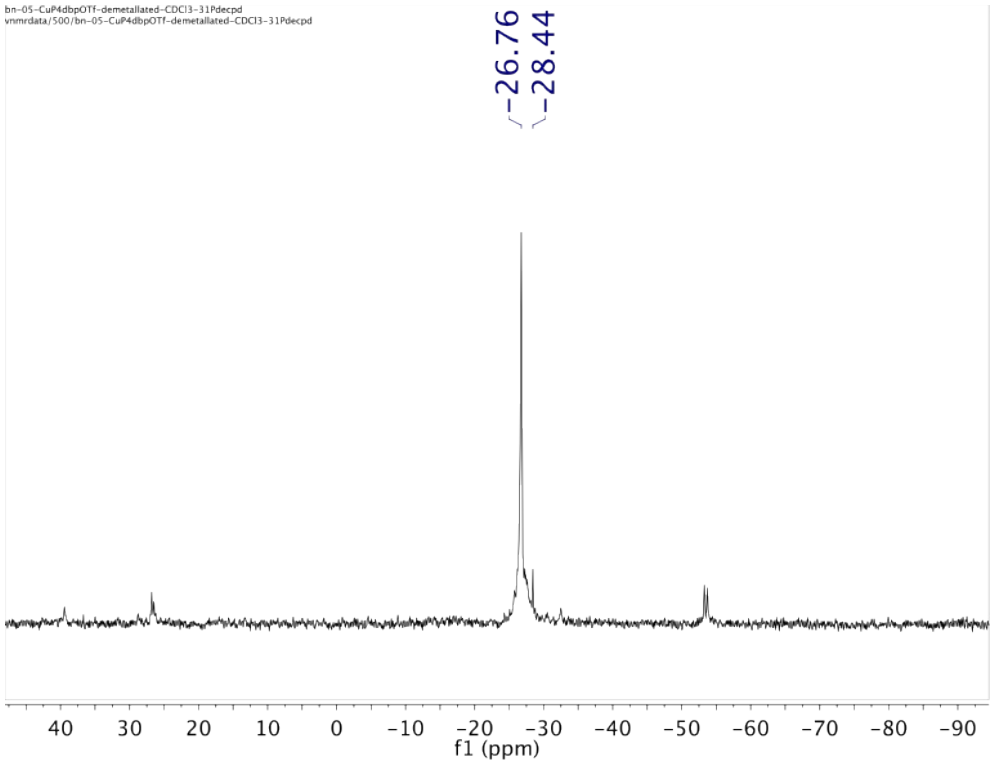

Figure S18. $^{31}P\{^{1}H\}$ NMR spectrum of **20**.

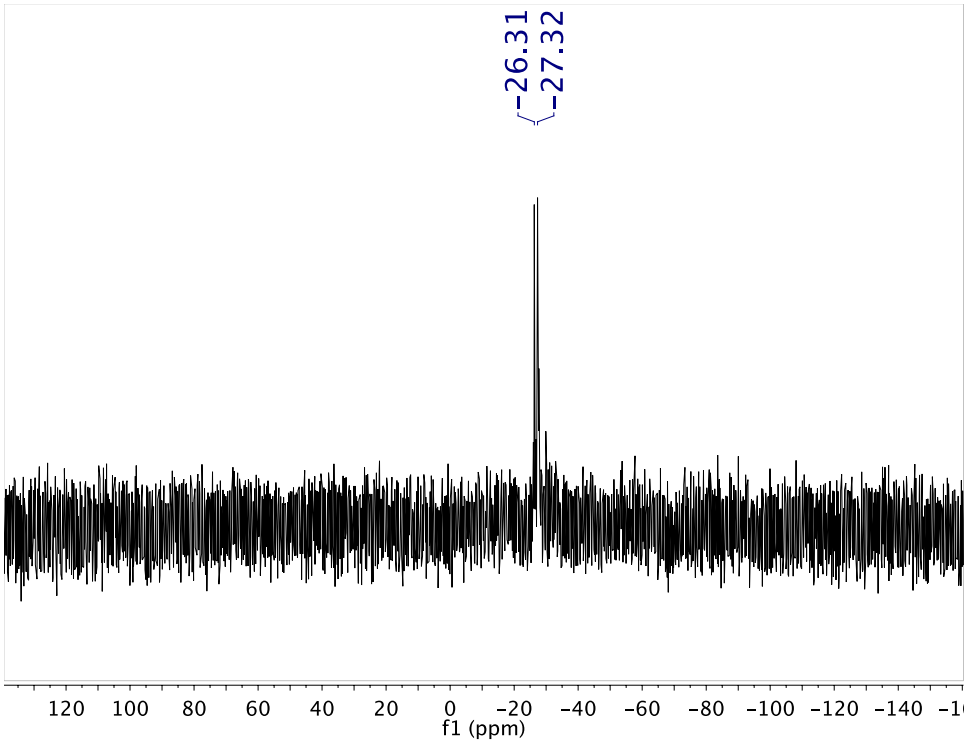

Figure S19. ^{31}P NMR spectrum of **21** in $CDCl_3$.

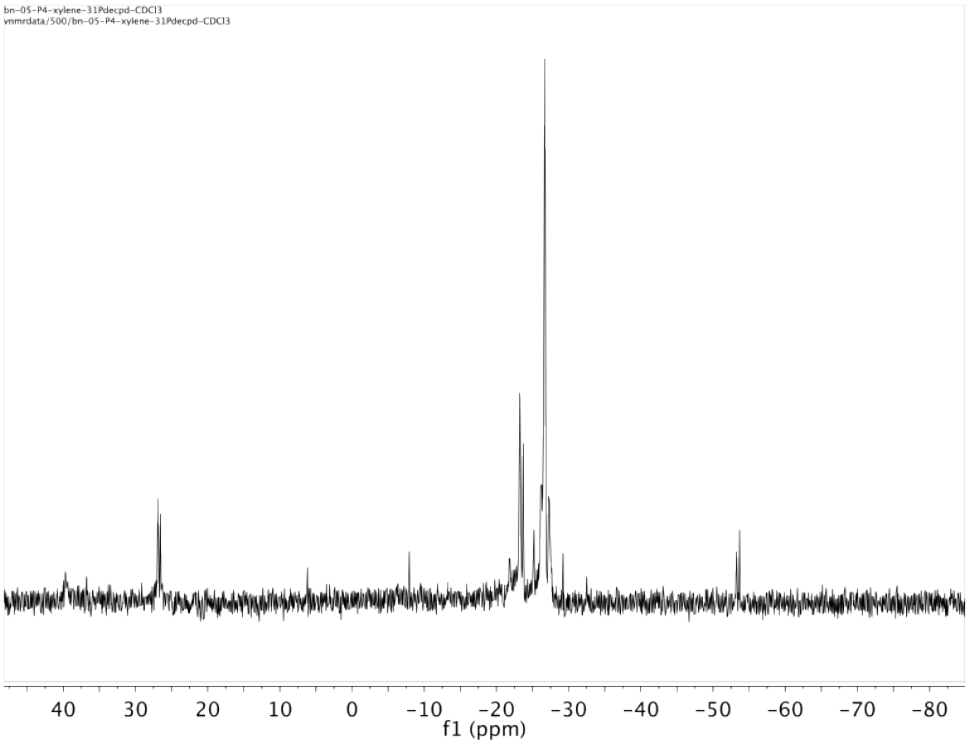

Figure S20. $^{31}P\{^{1}H\}$ NMR spectrum of **22**.

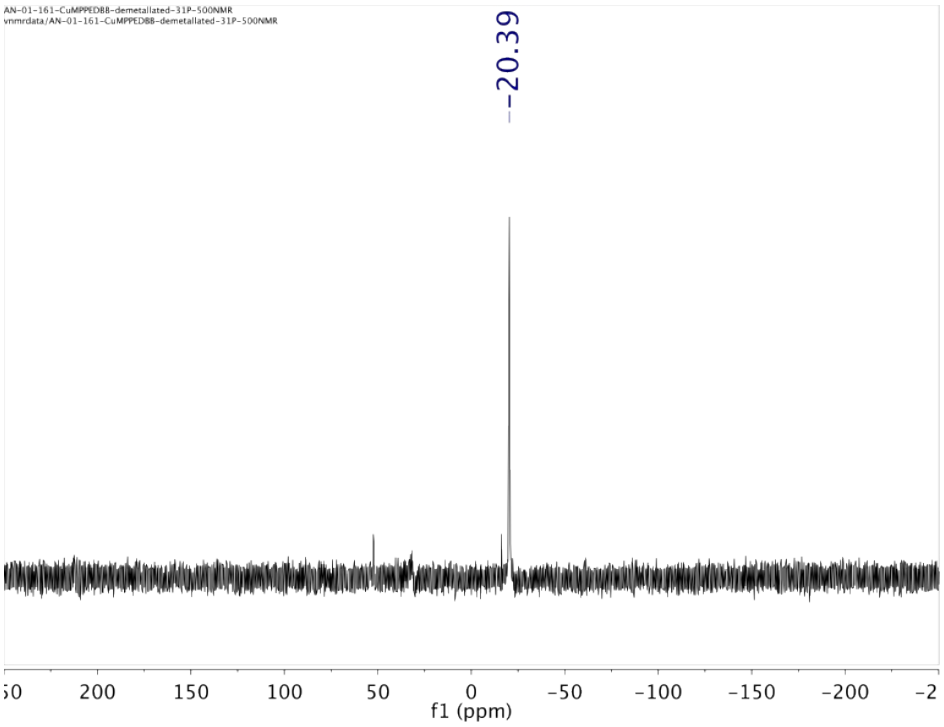

Figure S21. $^{31}P\{^{1}H\}$ NMR spectrum of **23**.

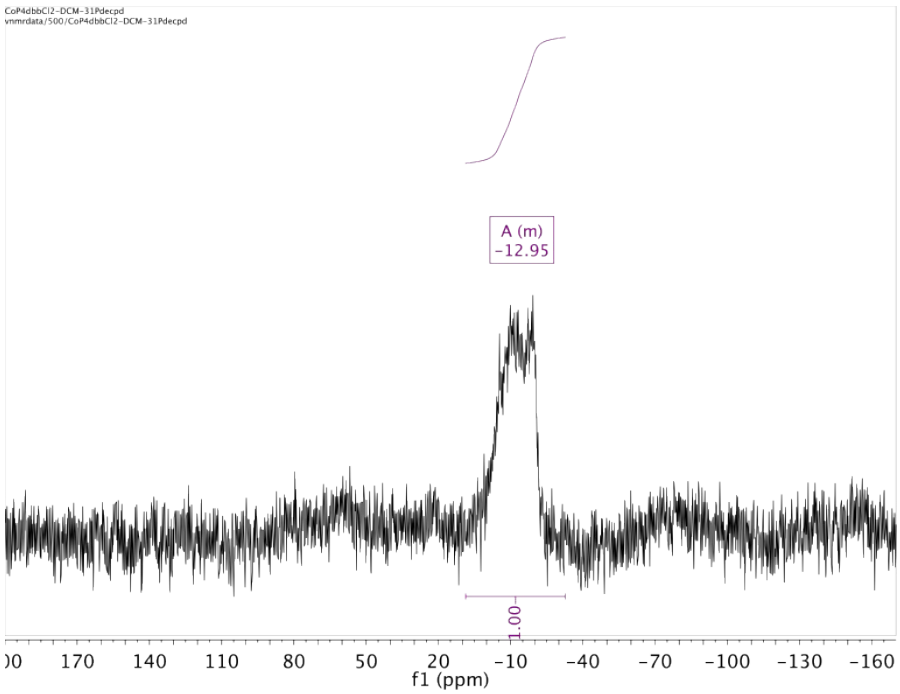

Figure S22. $^{31}P\{^{1}H\}$ NMR spectrum of Co(**23**)Cl_2.

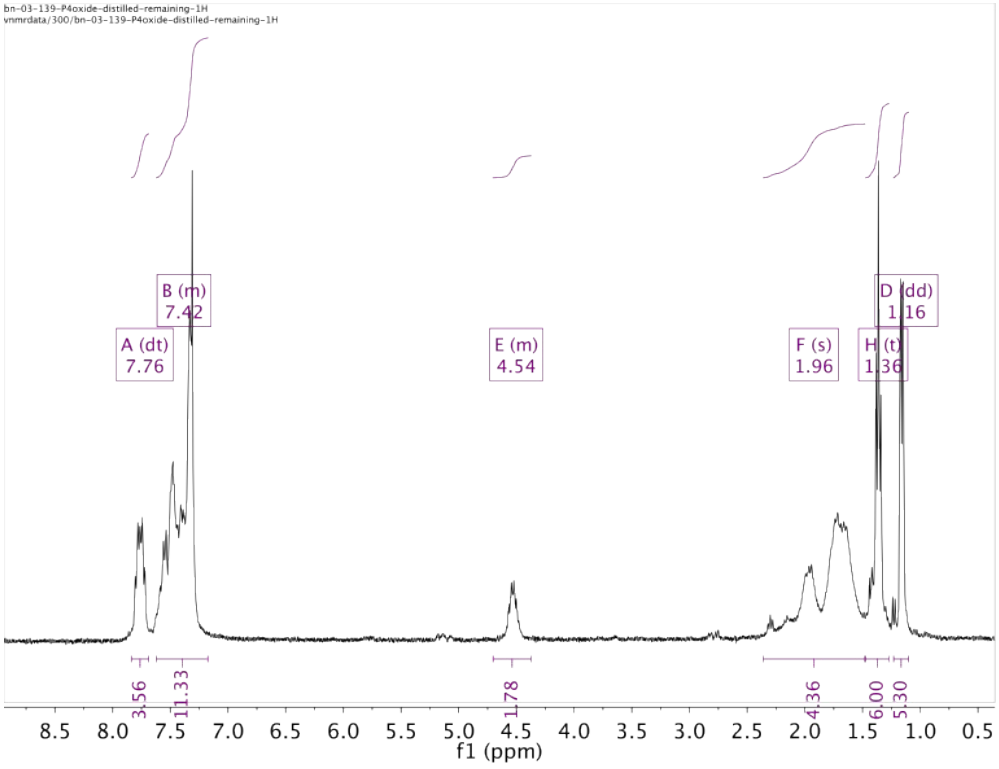

Figure S23. ^{1}H NMR spectrum of **3**.

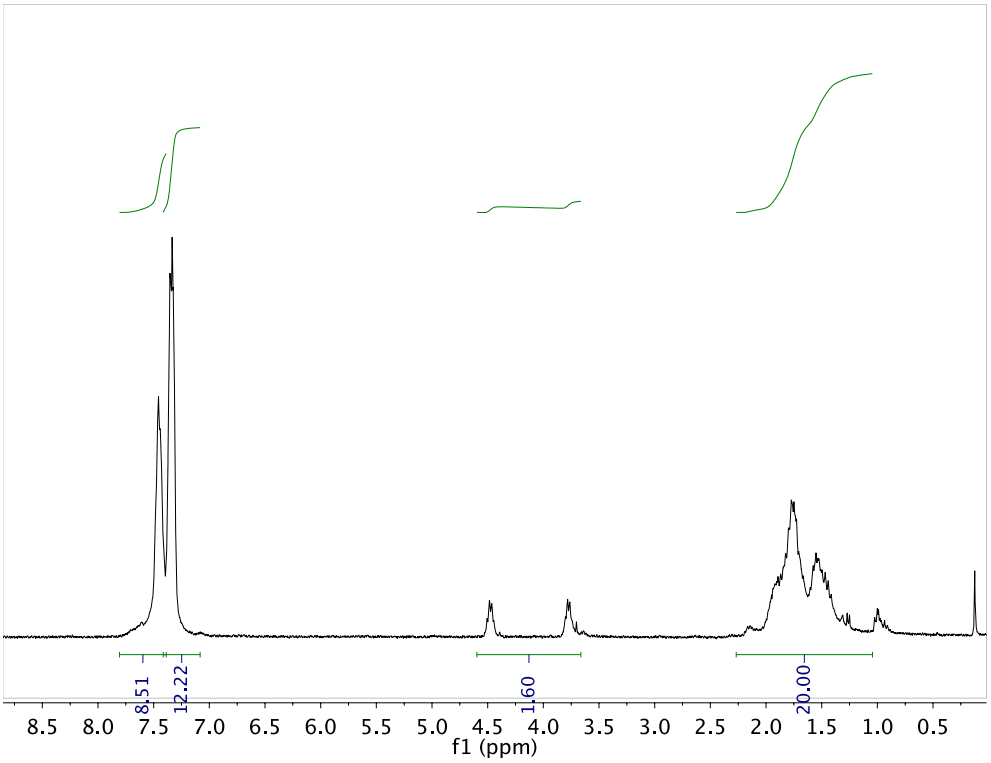

Figure S24. ^{1}H NMR spectrum of **4** in $CDCl_3$.

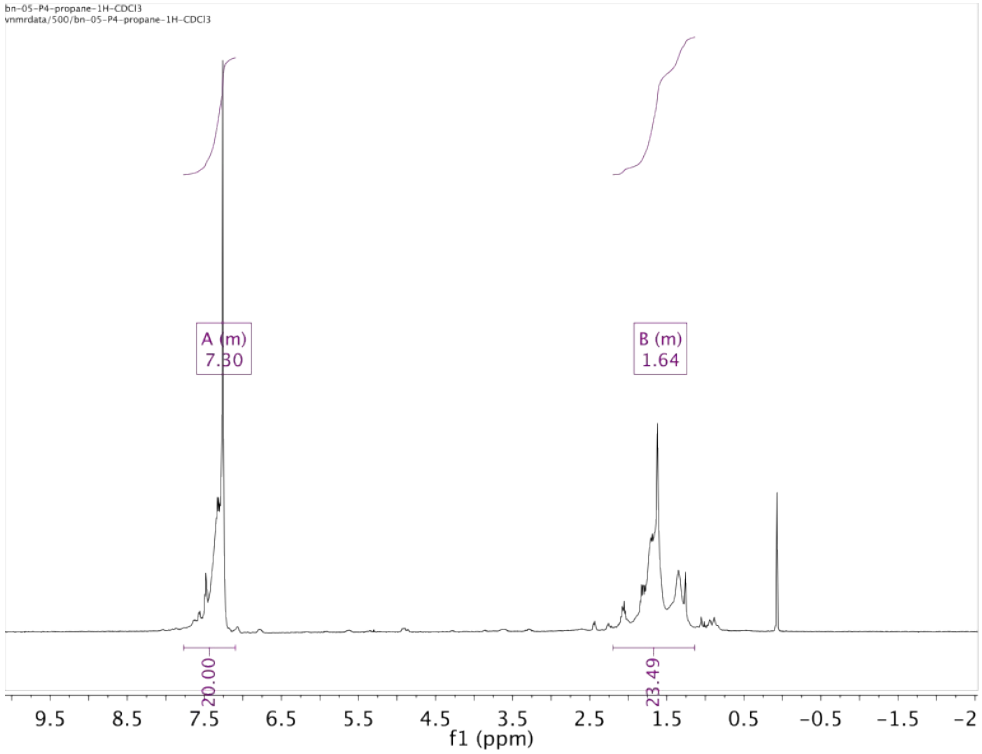

Figure S25. ^{1}H NMR spectrum of **20**.

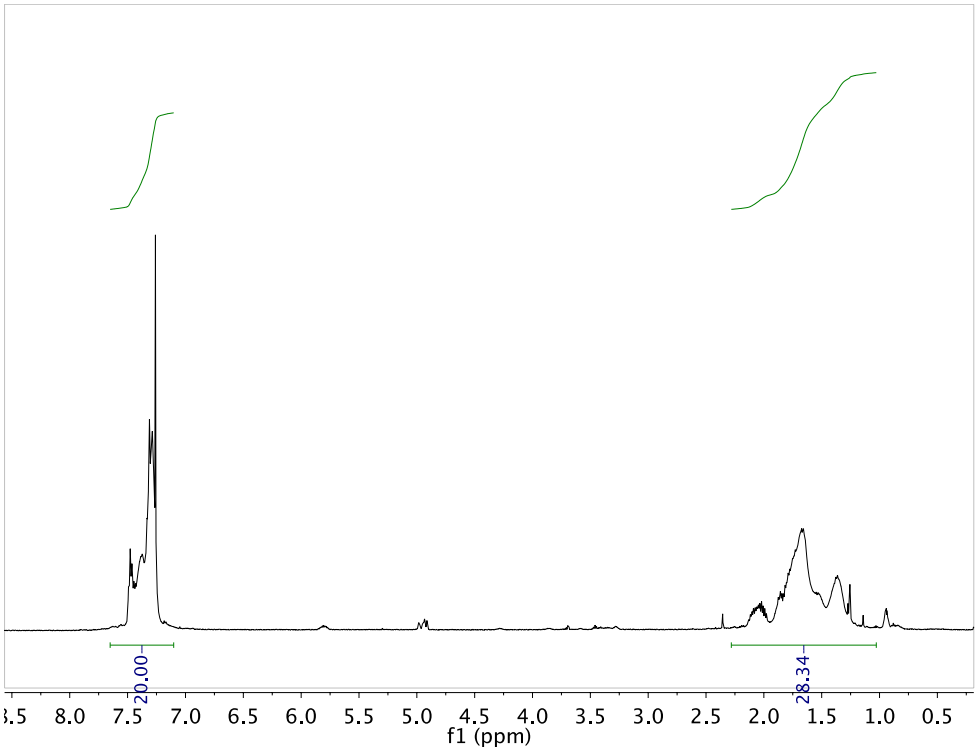

Figure S26. ^{1}H NMR spectrum of **21** in $CDCl_3$.

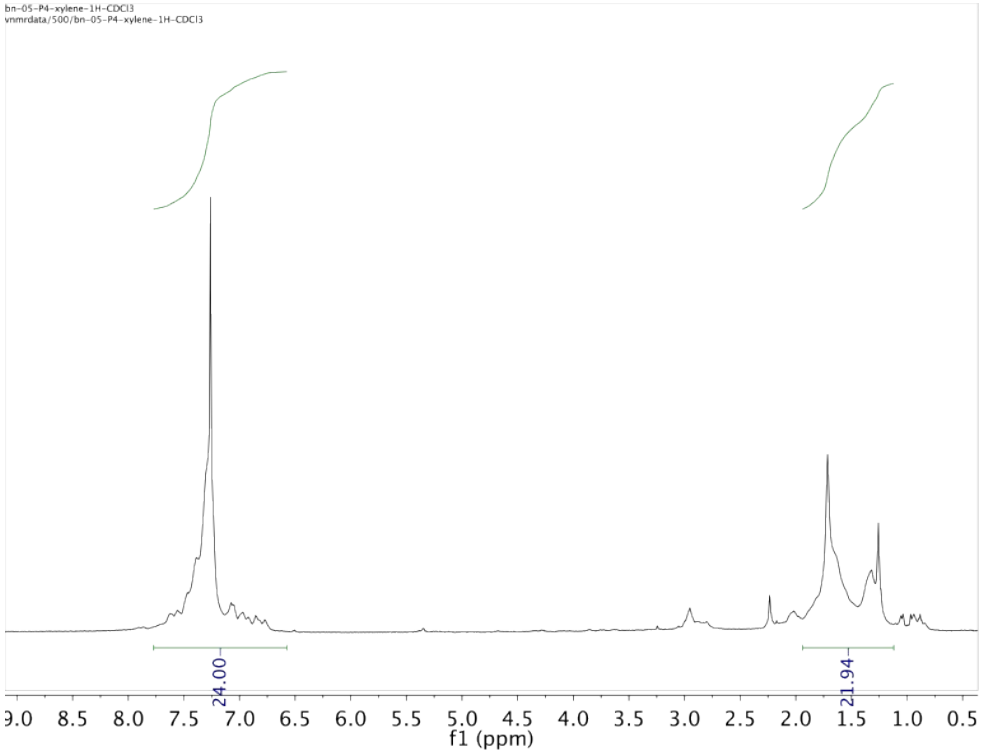

Figure S27. ^{1}H NMR spectrum of **22**.

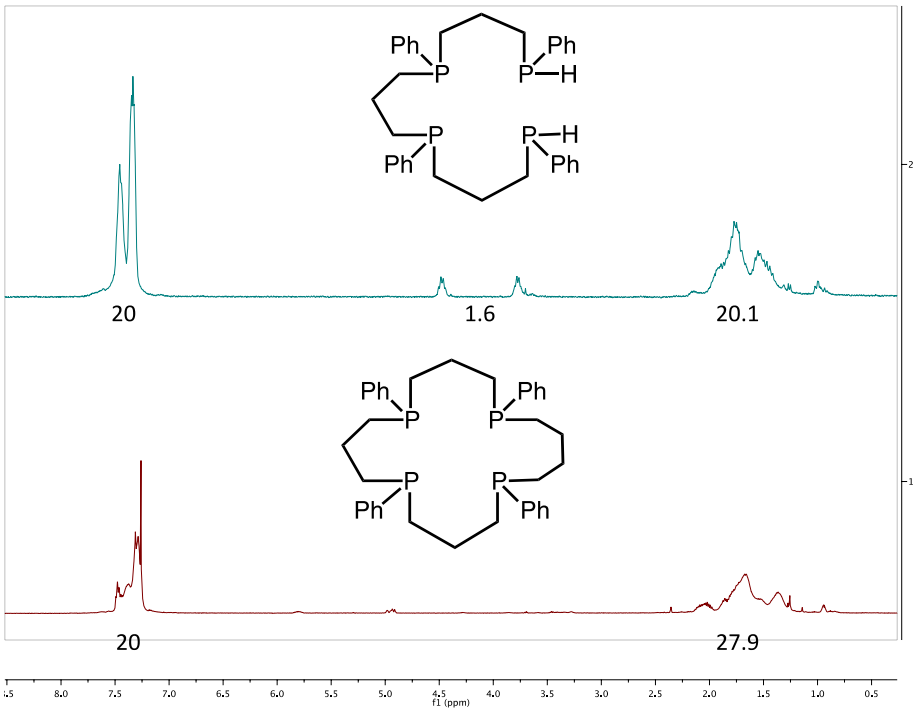

Figure S28. ^{1}H NMR spectrum of **11** vs. **21** in $CDCl_3$.

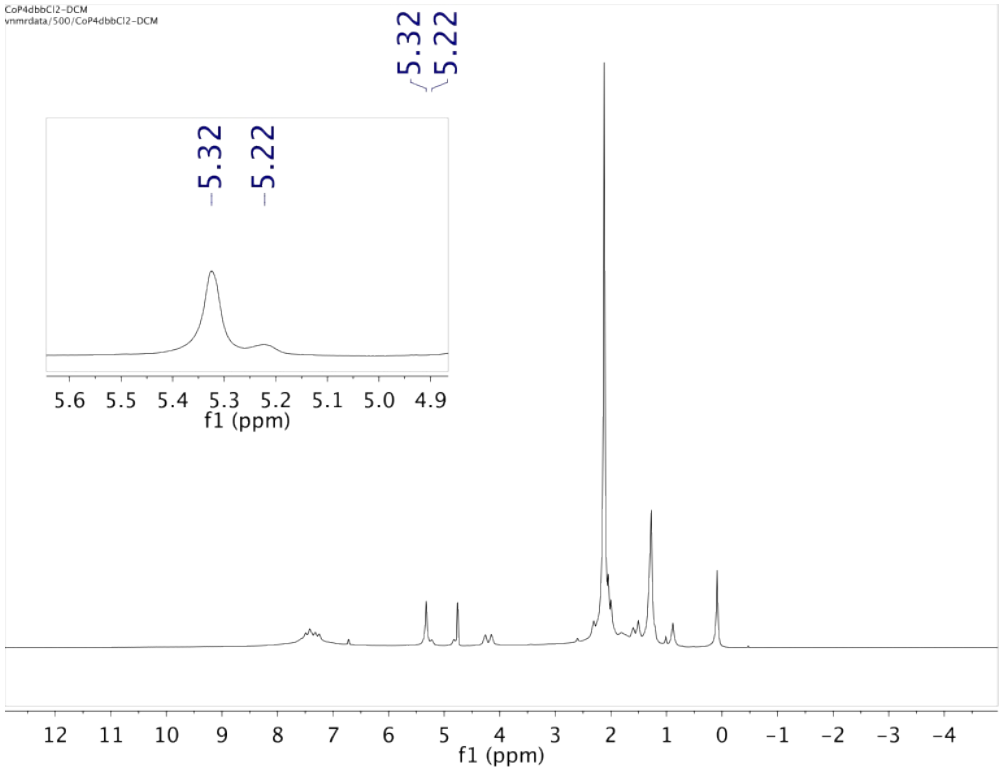

Figure S29. ^{1}H NMR spectrum of Co(**21**)Cl_2 for Evans' method.

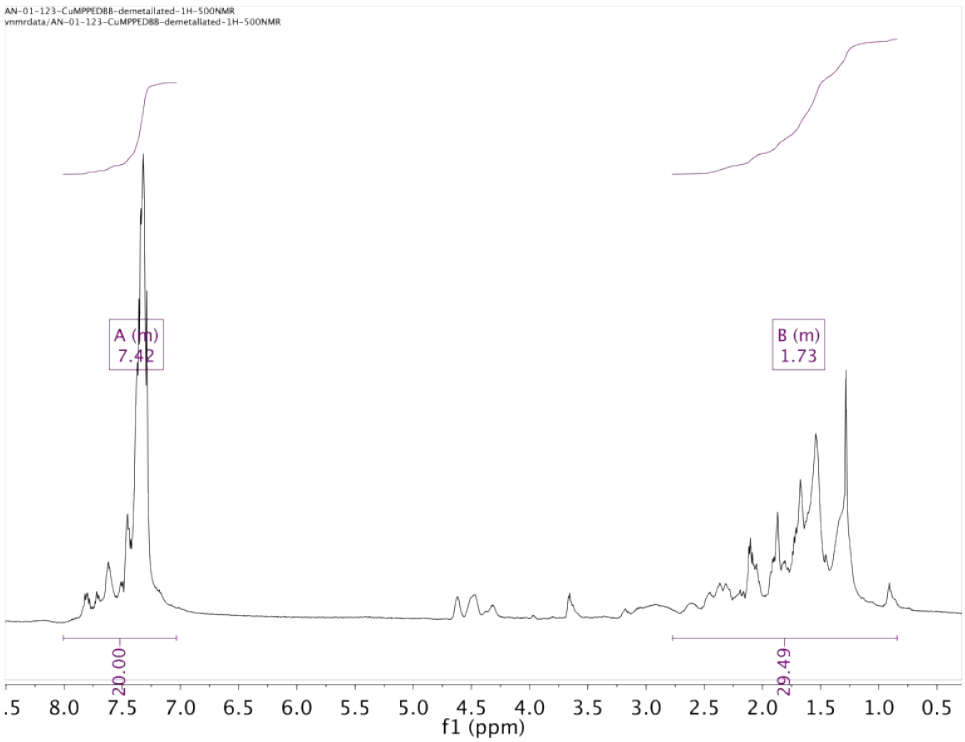

Figure S30. ^{1}H NMR spectrum of **23**.

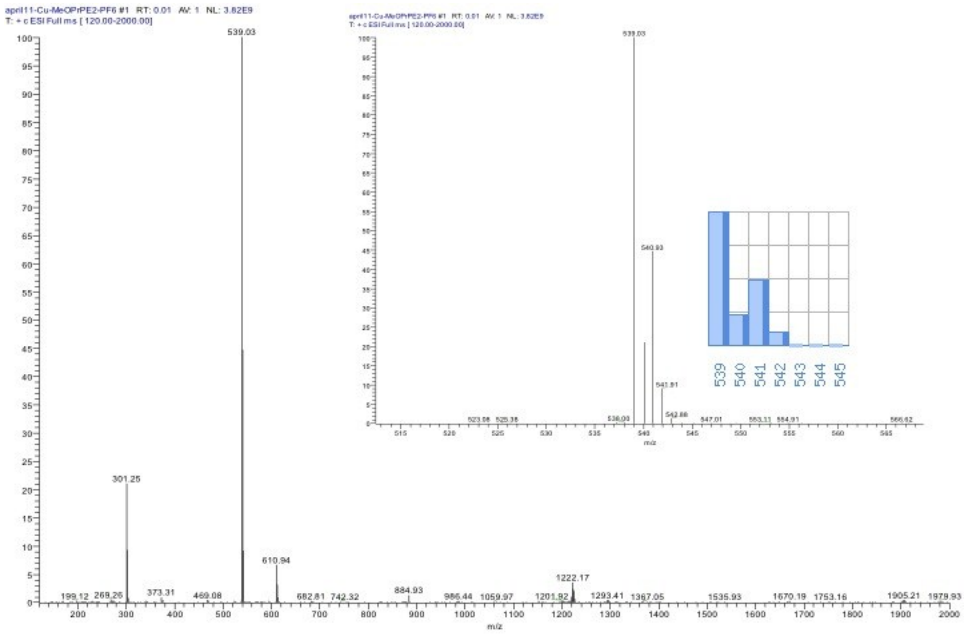

Figure S31. ESI-MS of $Cu(MeOPrPE)_2PF_6$ (**7**).

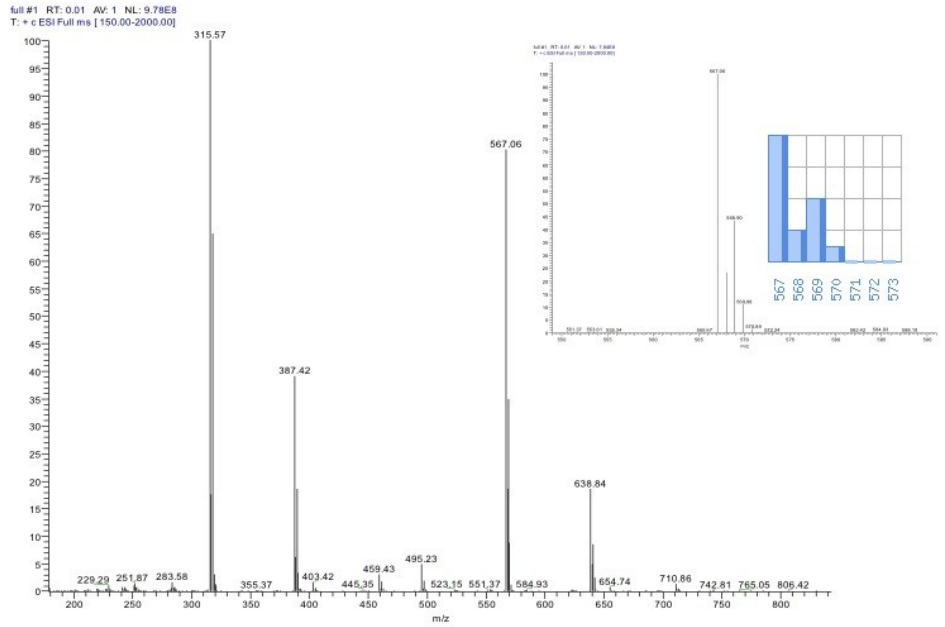

Figure S32. ESI-MS of $Cu(MeOPrPP)_2OTf$ (**8**).

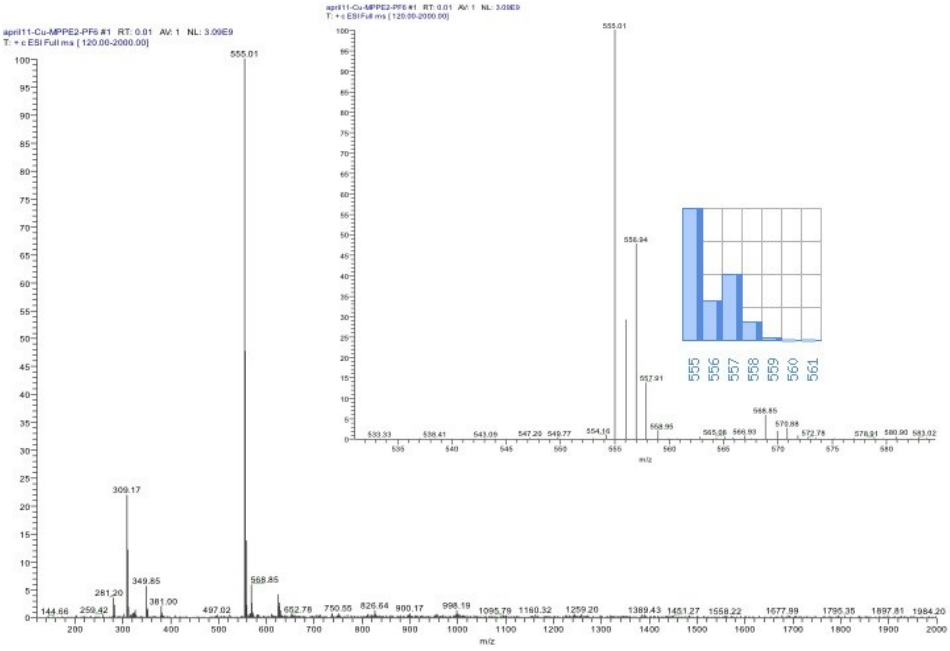

Figure S33. ESI-MS of $Cu(MPPE)_2PF_6$ (**9**).

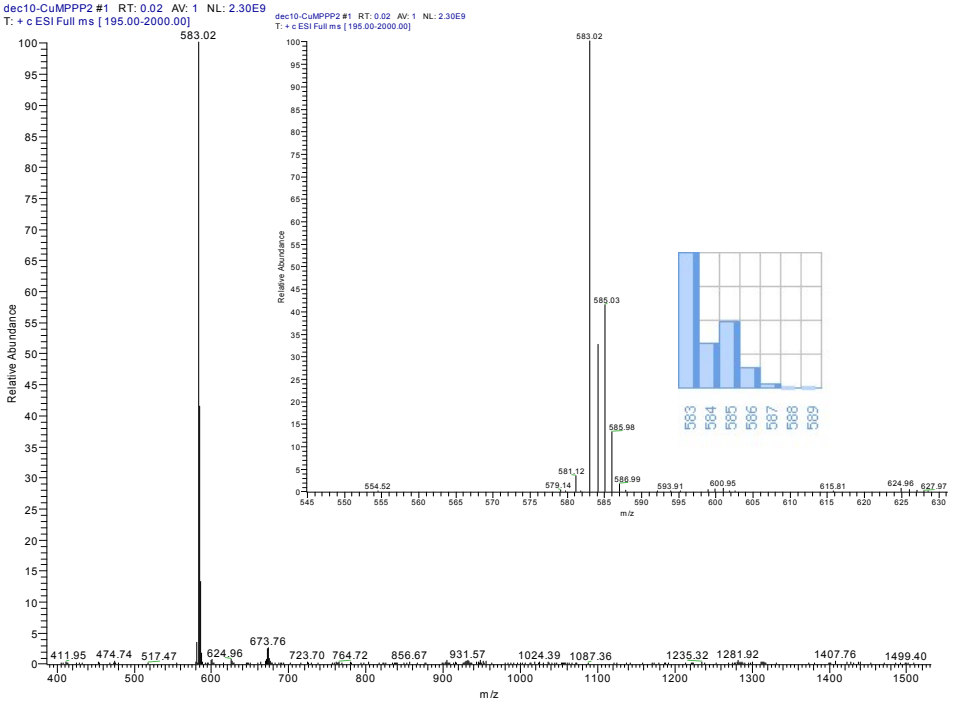

Figure S34. ESI-MS of Cu(MPPP)$_2$OTf (**10**).

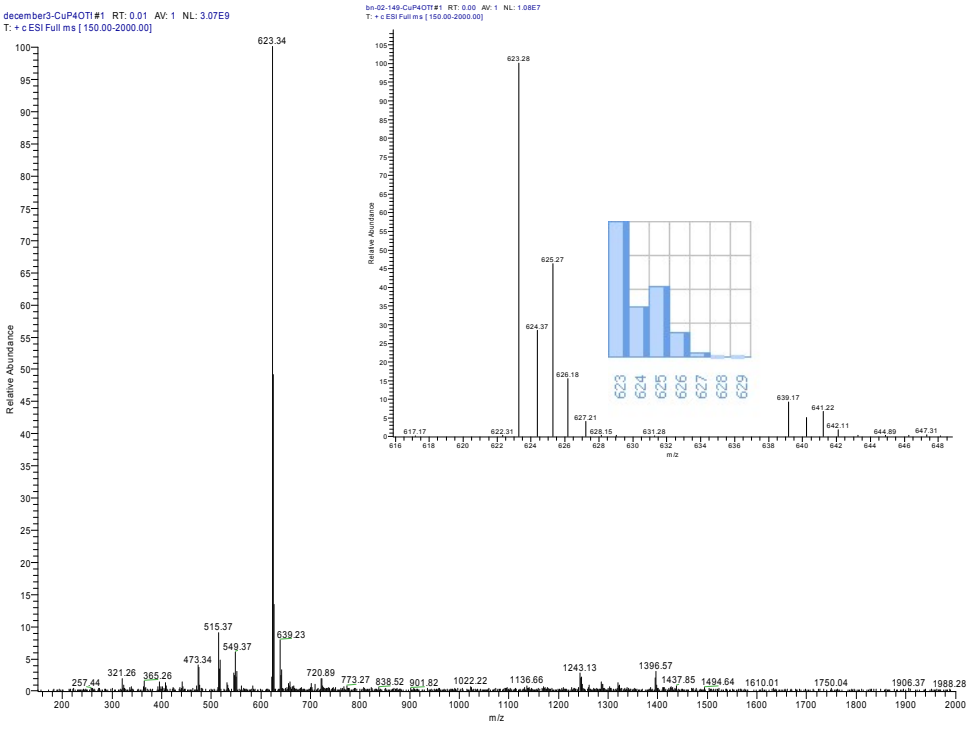

Figure S35. ESI-MS of Cu(**4**)OTf (**11**).

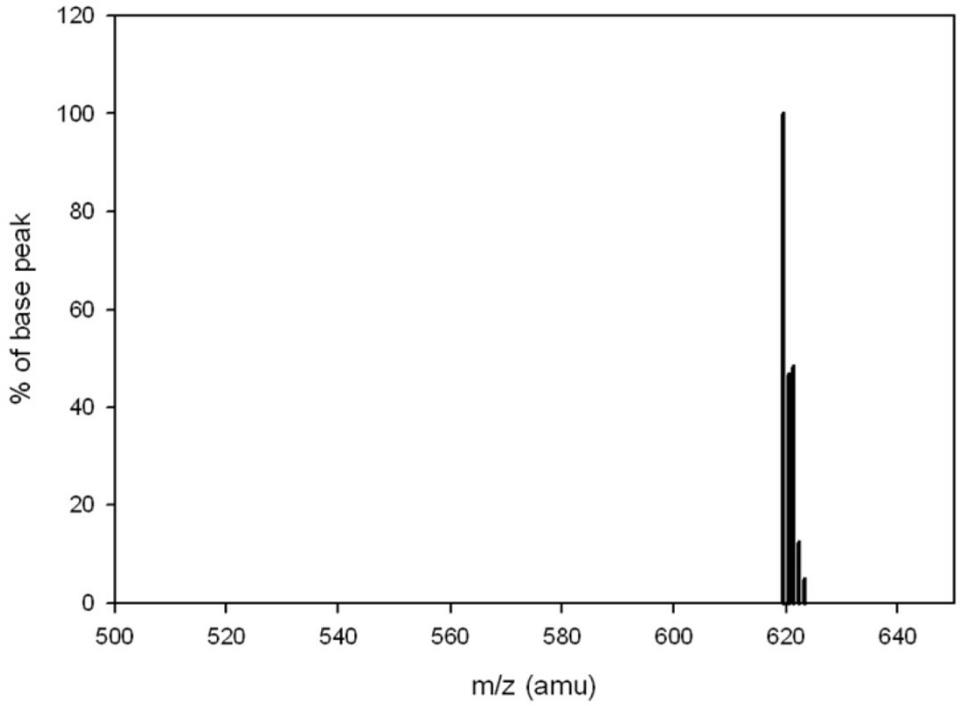

Figure S36. ESI mass spectrum of **12**.

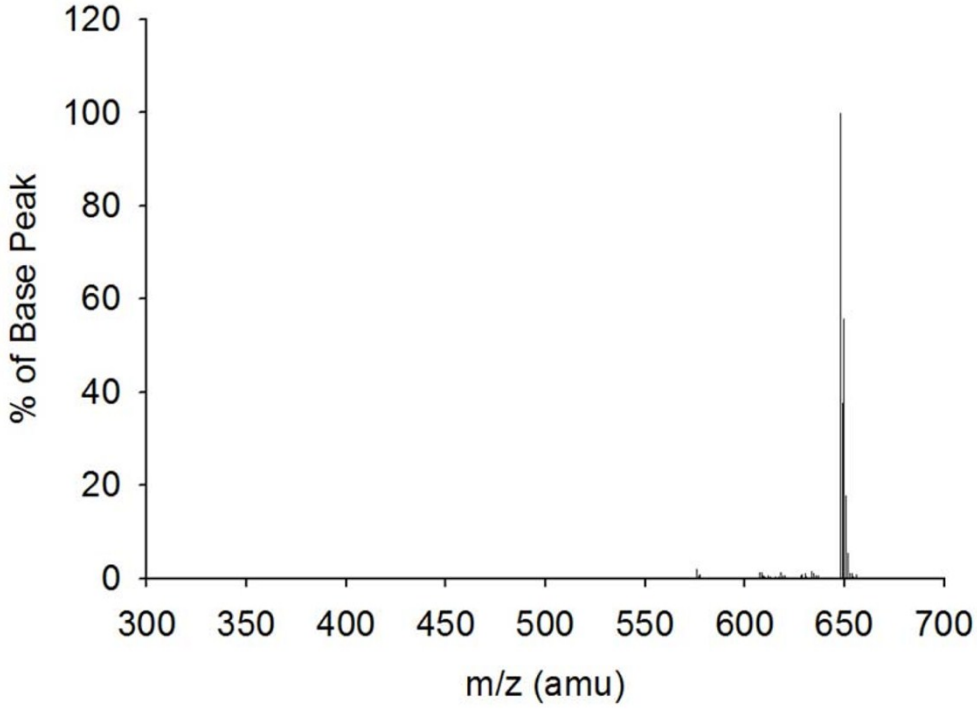

Figure S37. ESI mass spectrum of **13**.

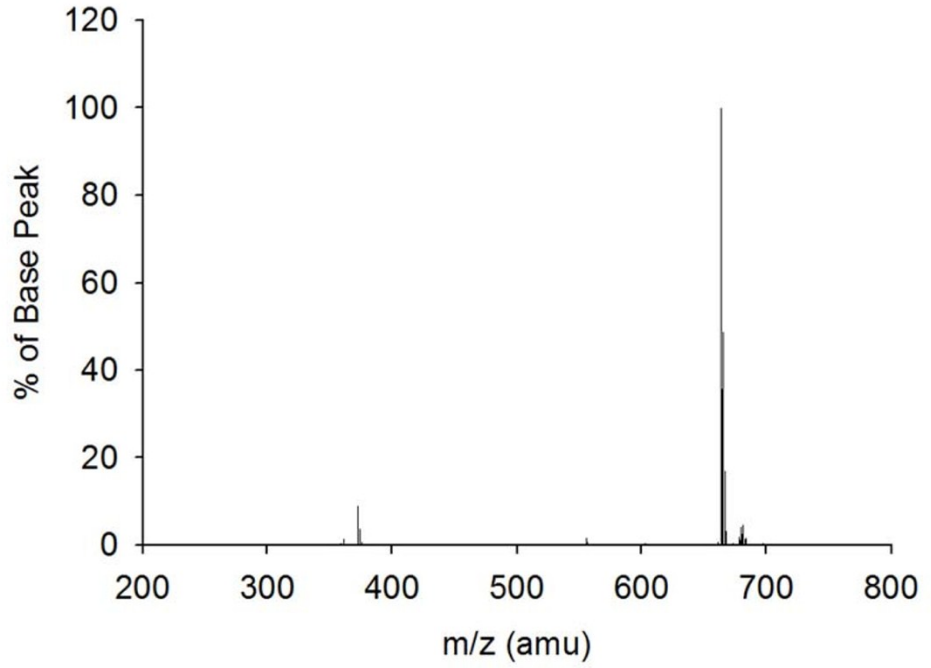

Figure S38. ESI mass spectrum of **15**.

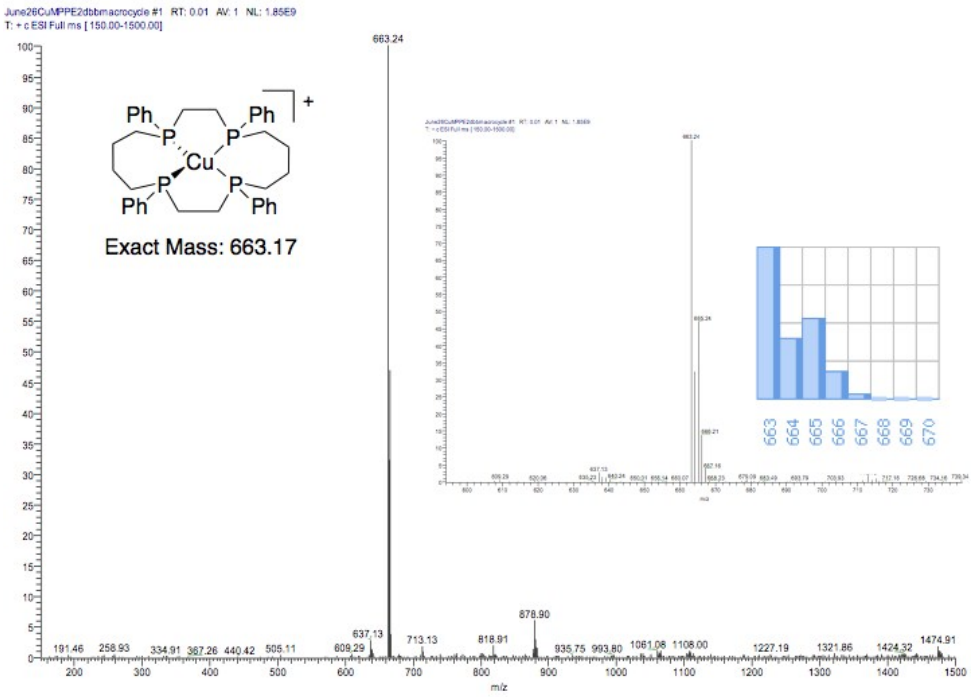

Figure S39. ESI mass spectrum of **16**.

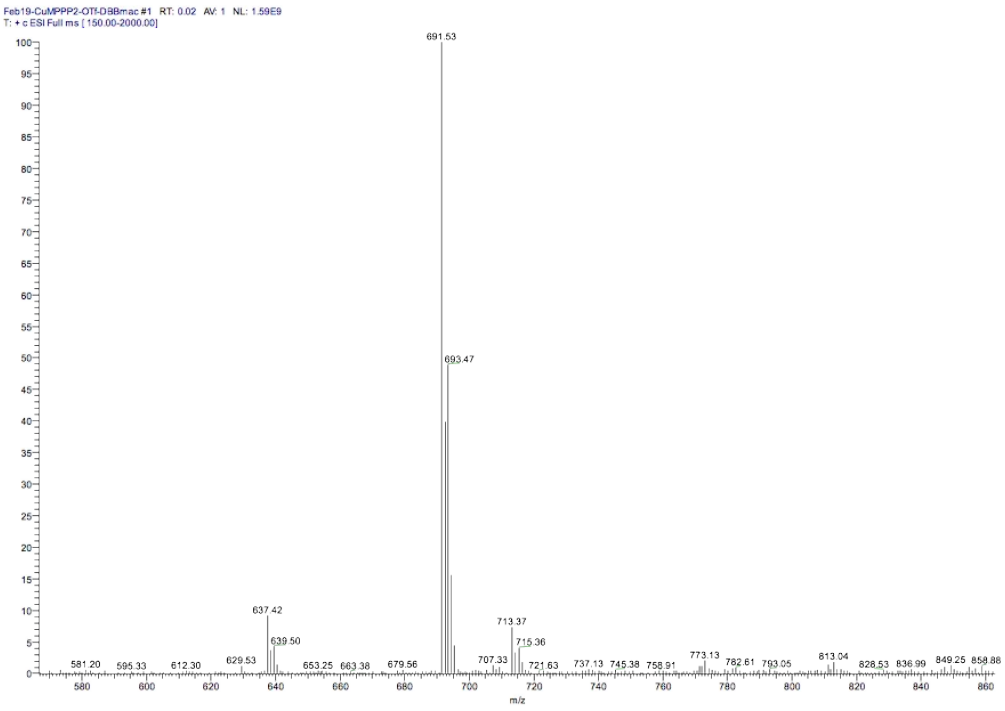

Figure S40. ESI mass spectrum of **17**.

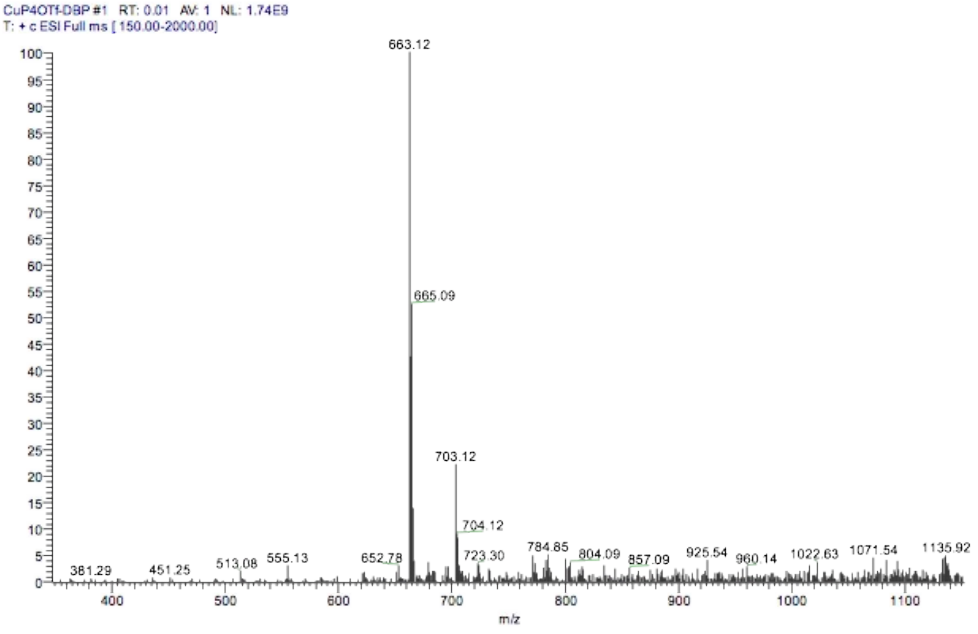

Figure S41. ESI mass spectrum of **15.**

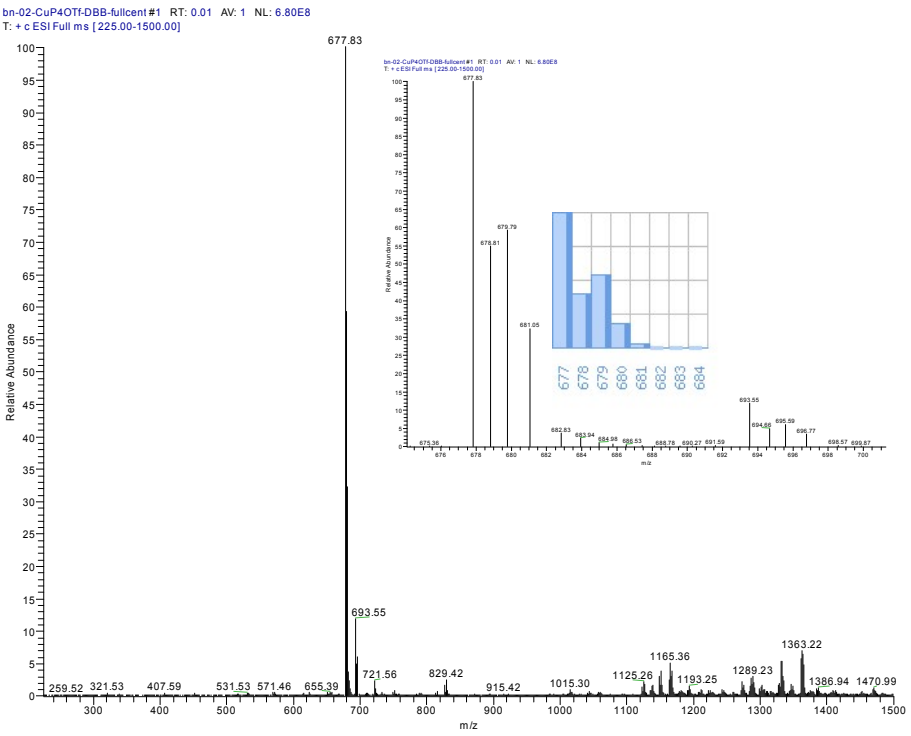

Figure S42. ESI-MS of **18**.

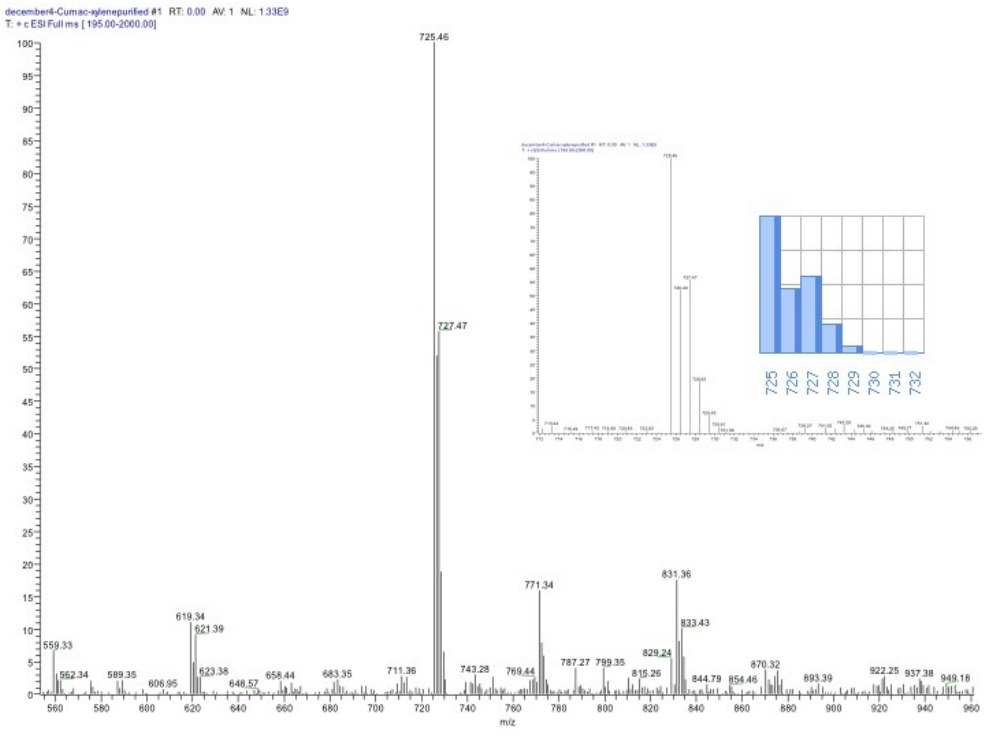

Figure S43. ESI-MS of **19**.

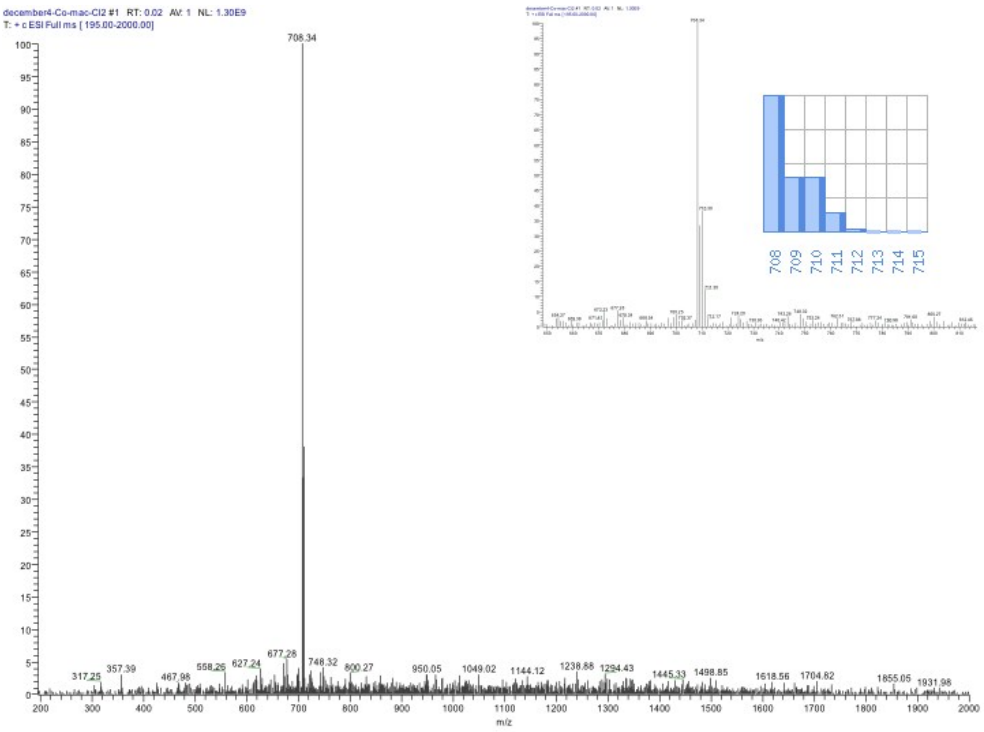

Figure S44. ESI-MS of [Co(**21**)]Cl_2.

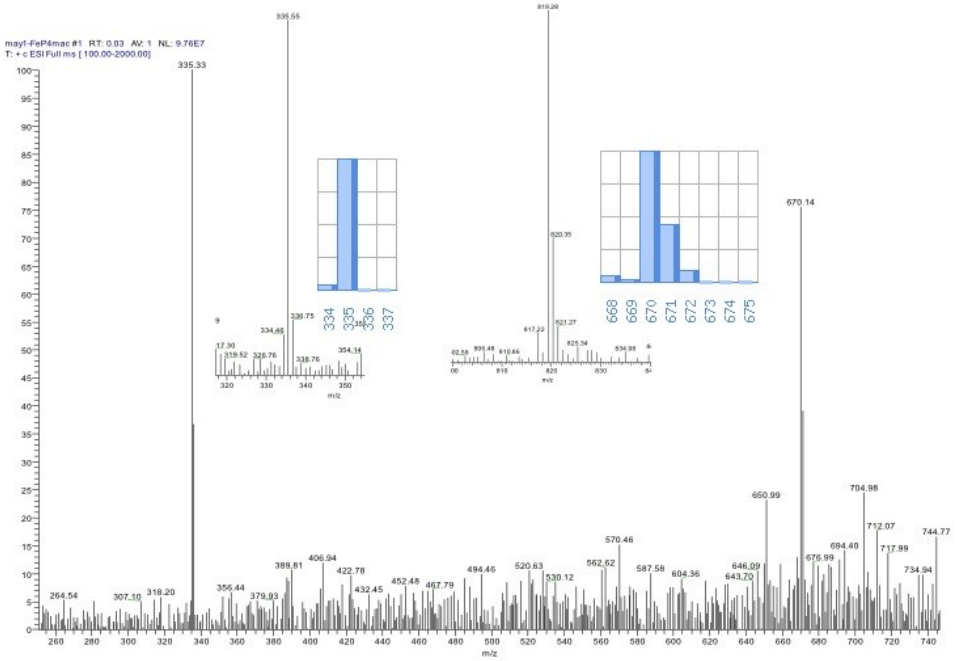

Figure S45. ESI-MS of **[**Fe(**21**)$(CH_3CN)_2$]$(BPh_4)_2$.

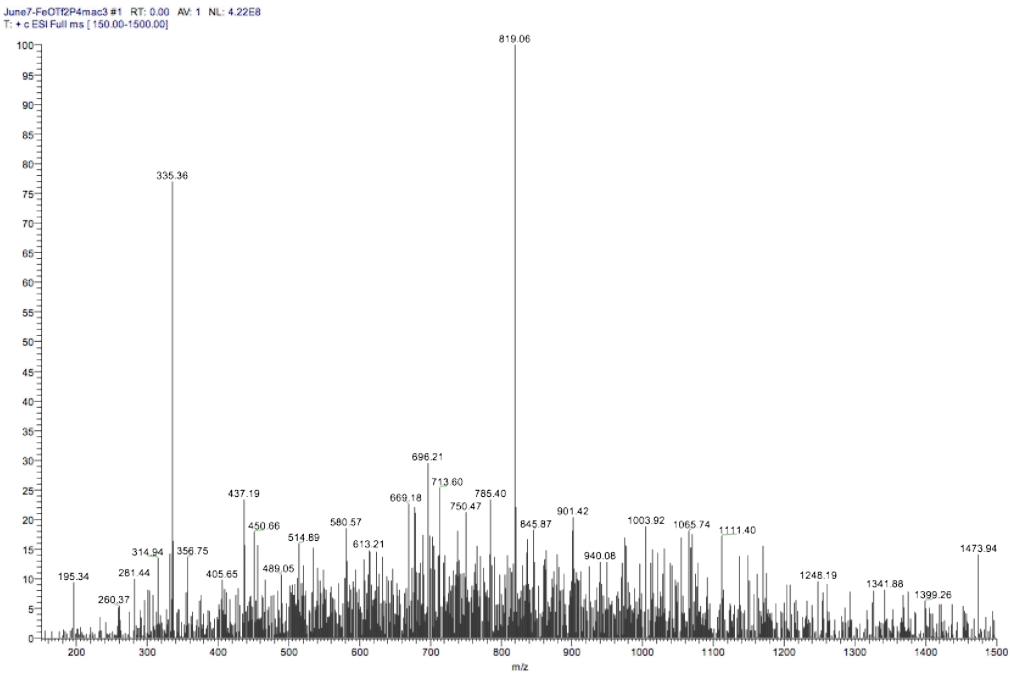

Figure S46. ESI mass spectrum of [Fe(**21**)$(CH_3CN)_2$]$(OTf)_2$. The peak at m/z 819 is Fe(**21**)OTf]$^+$ and the peak at 335 is [Fe(**21**)]$^{2+}$.

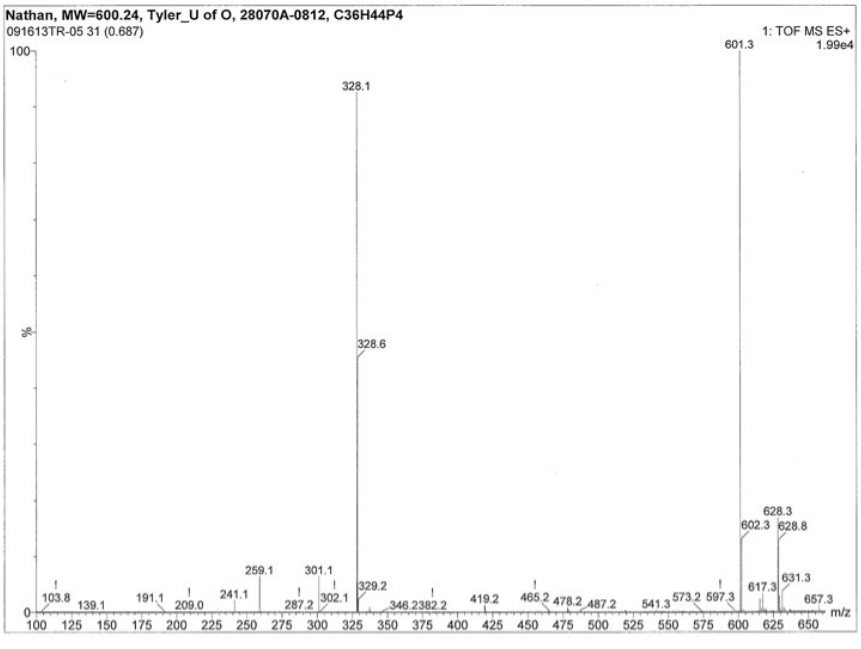

Figure S47. FAB mass spectrum of **23**.

Elemental Composition Report **Page 1**

Single Mass Analysis
Tolerance = 50.0 PPM / DBE: min = -1.5, max = 50.0
Selected filters: None

Monoisotopic Mass, Even Electron Ions
8 formula(e) evaluated with 1 results within limits (up to 50 best isotopic matches for each mass)
Elements Used:
C: 0-36 H: 0-45 Na: 0-1 P: 0-4

Nathan, MW=600.24, Tyler_U of O, 28070A-0812, C36H44P4
091613TR-05 36 (0.793) Cm (36:48)

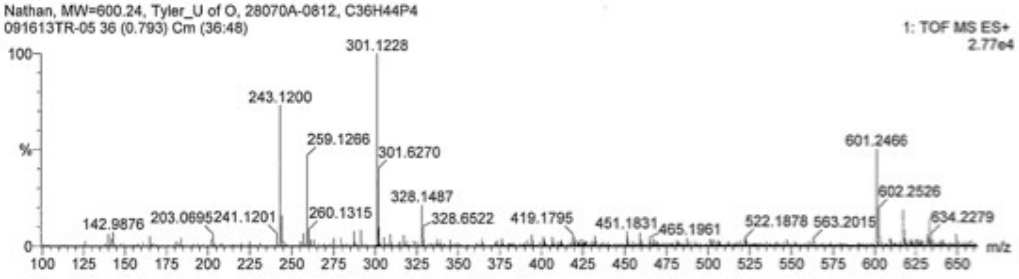

Minimum:				-1.5		
Maximum:		5.0	50.0	50.0		
Mass	Calc. Mass	mDa	PPM	DBE	i-FIT	Formula
601.2466	601.2472	-0.6	-1.0	16.5	43.1	C36 H45 P4

Figure S48. Hi-Res FAB-MS of **23**.

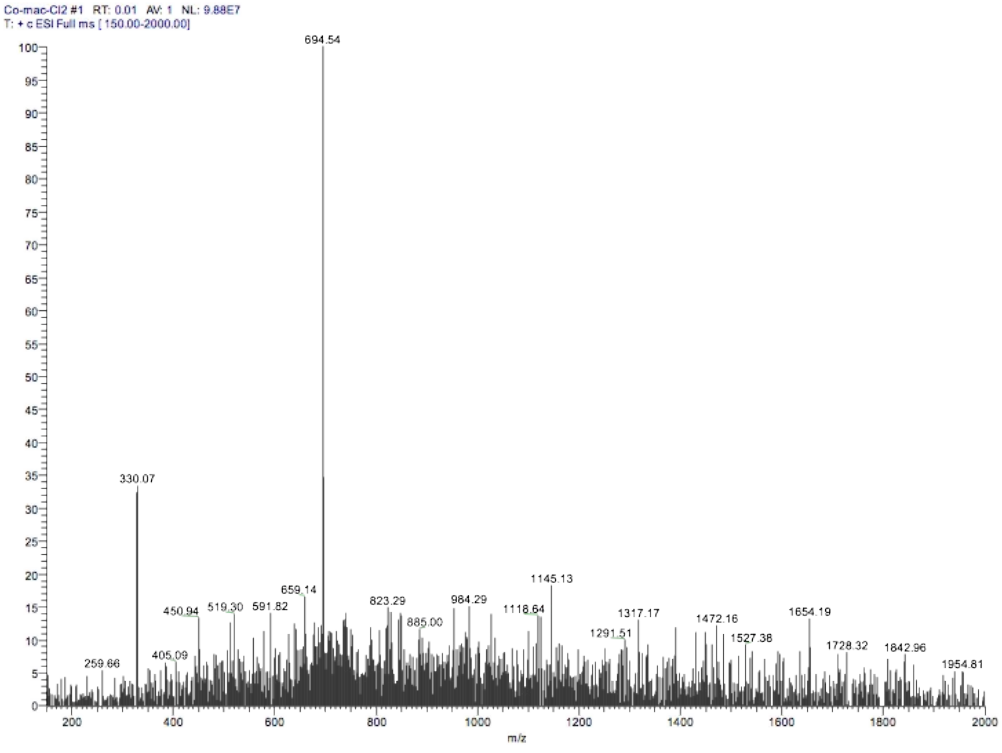

Figure S49. ESI mass spectrum of Co(**23**)Cl_2.

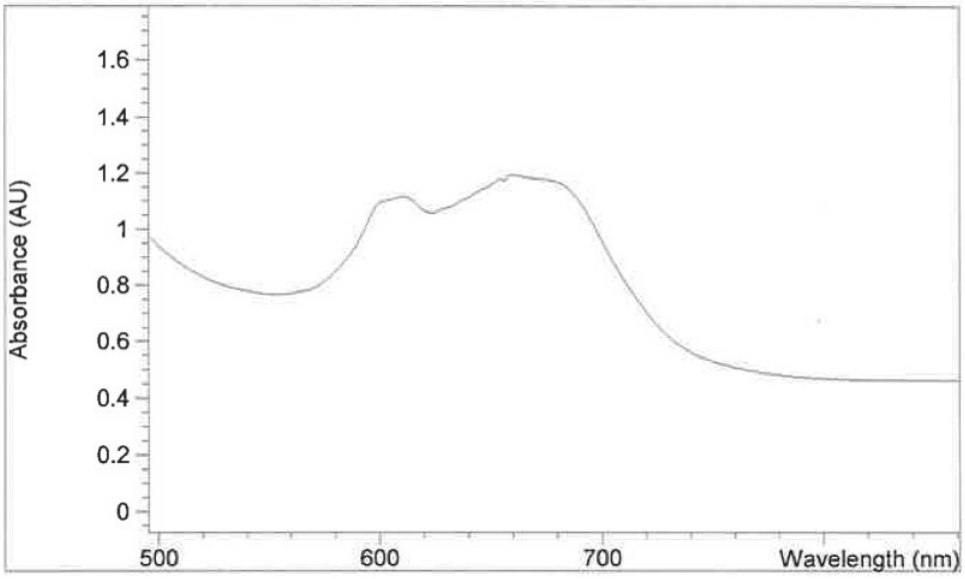

Figure S50. UV-Vis spectrum of Co(**21**)Cl_2 in dichloromethane.

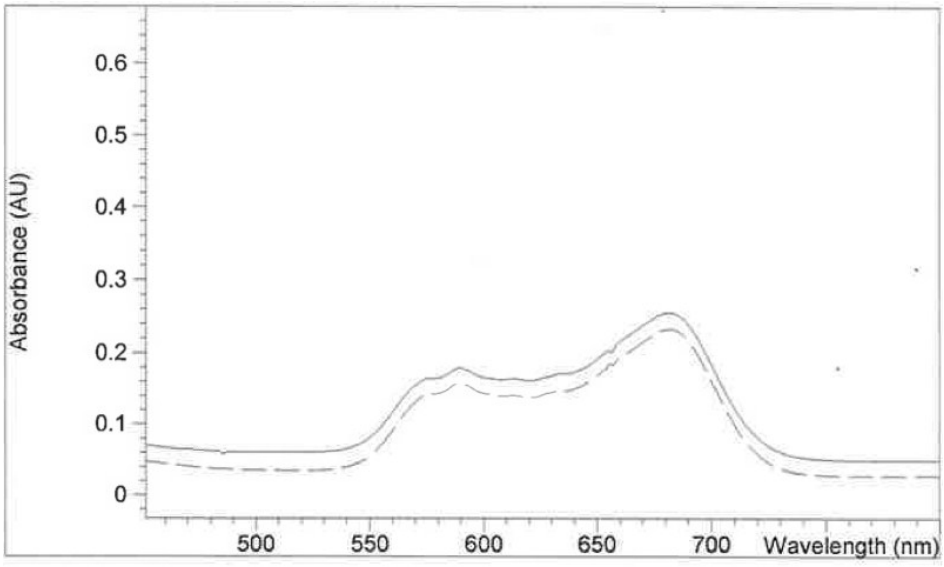

Figure S51. UV-Vis spectrum of Co(**23**)Cl_2 in dichloromethane.

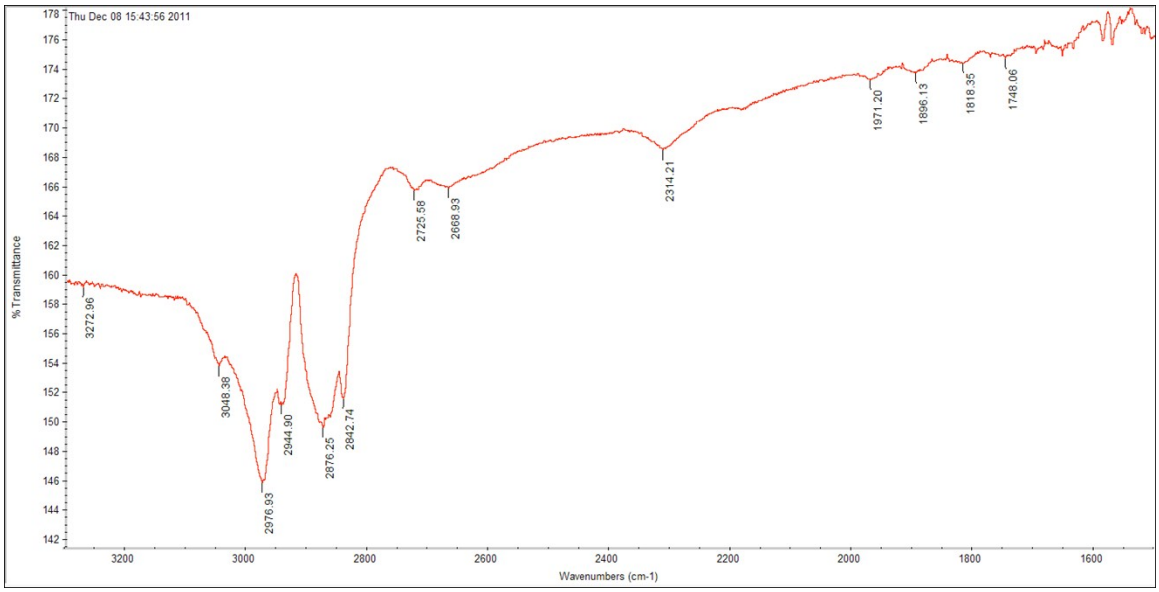

Figure S52. Infrared spectrum (ATR method) of Cu(**4**)OTf, **11**.

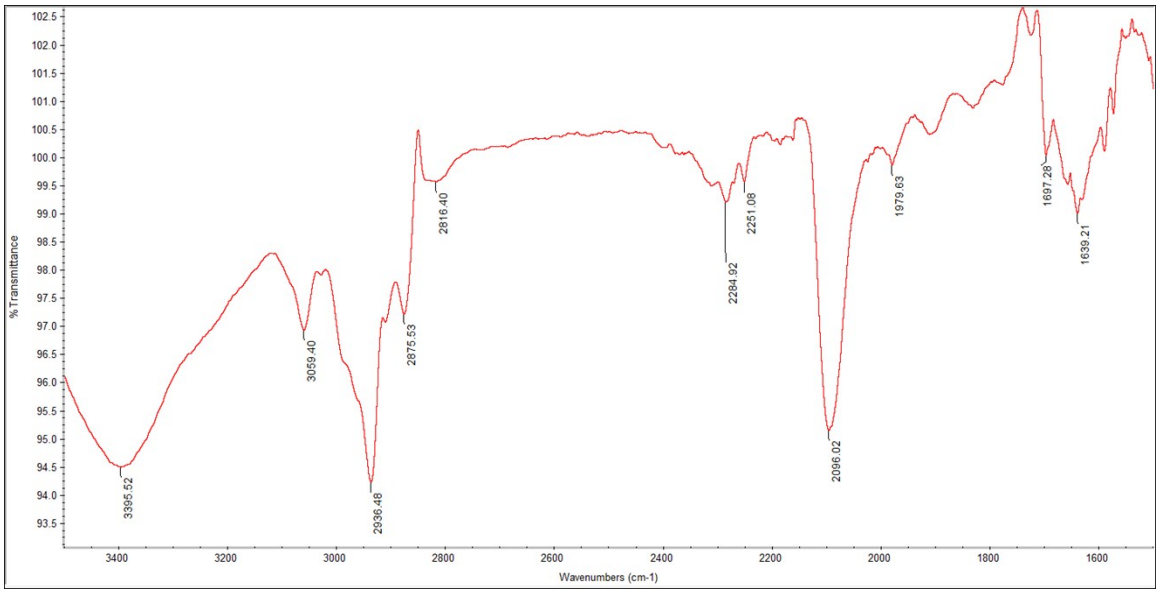

Figure S53. Infrared spectrum (ATR method) of [Fe(**21**)$(CH_3CN)_2$]$(OTf)_2$.

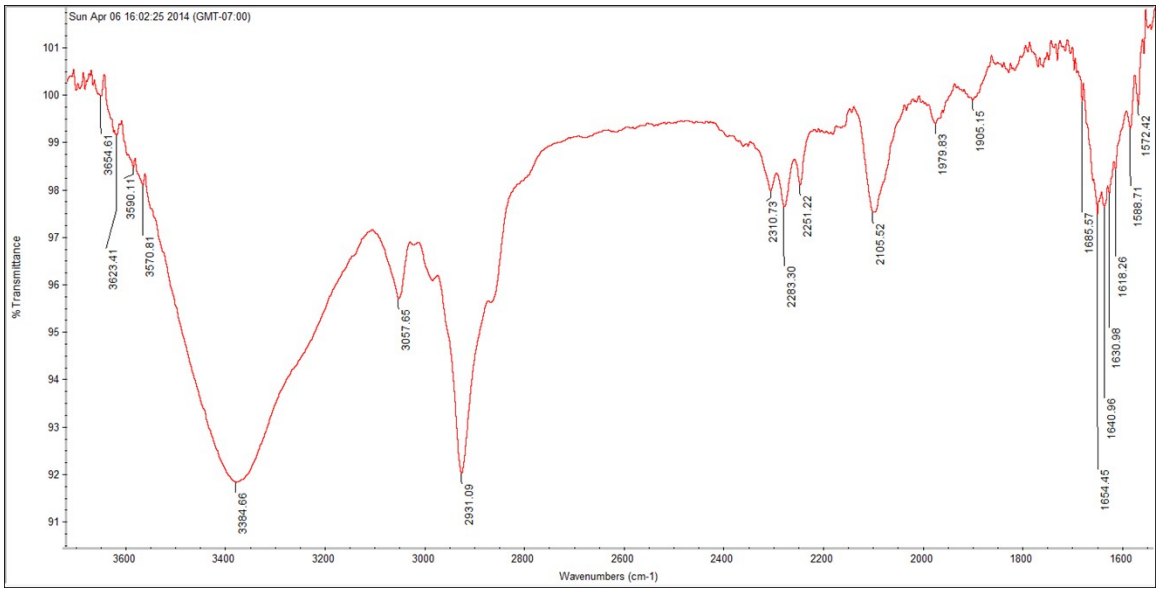

Figure S54. Infrared spectrum (ATR method) of [Fe(**21**)(CH_3CN)$_2$](OTf)$_2$ prepared in an Ar-filled glovebox.

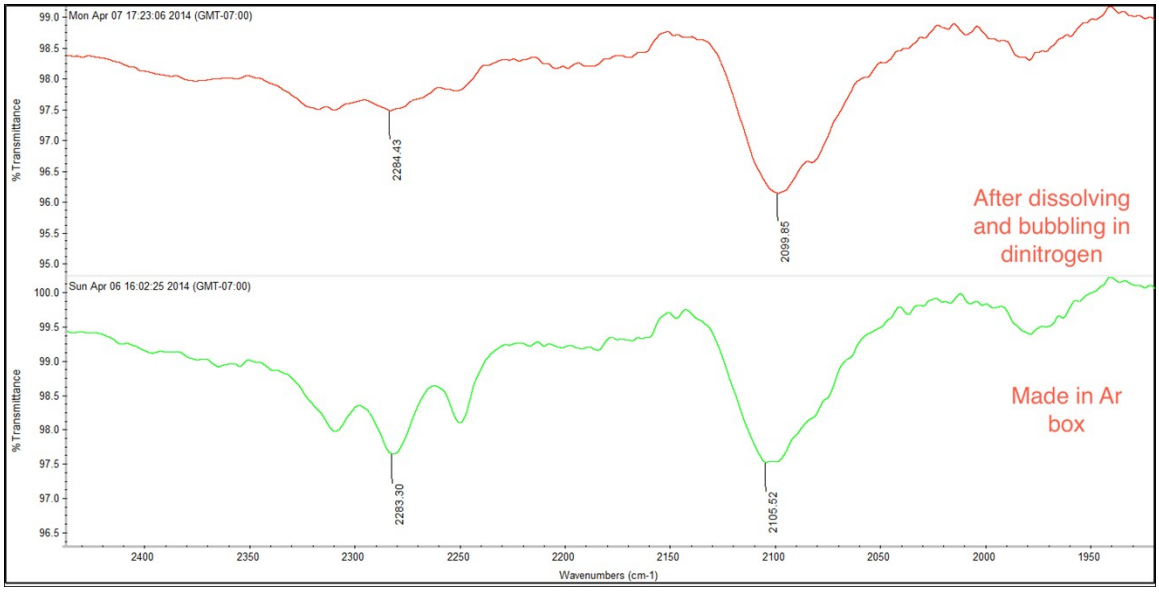

Figure S55. Infrared spectrum (ATR method) of [Fe(**21**)(CH_3CN)$_2$](OTf)$_2$ prepared in an Ar-filled glovebox, redissolved and and bubbled with N_2.

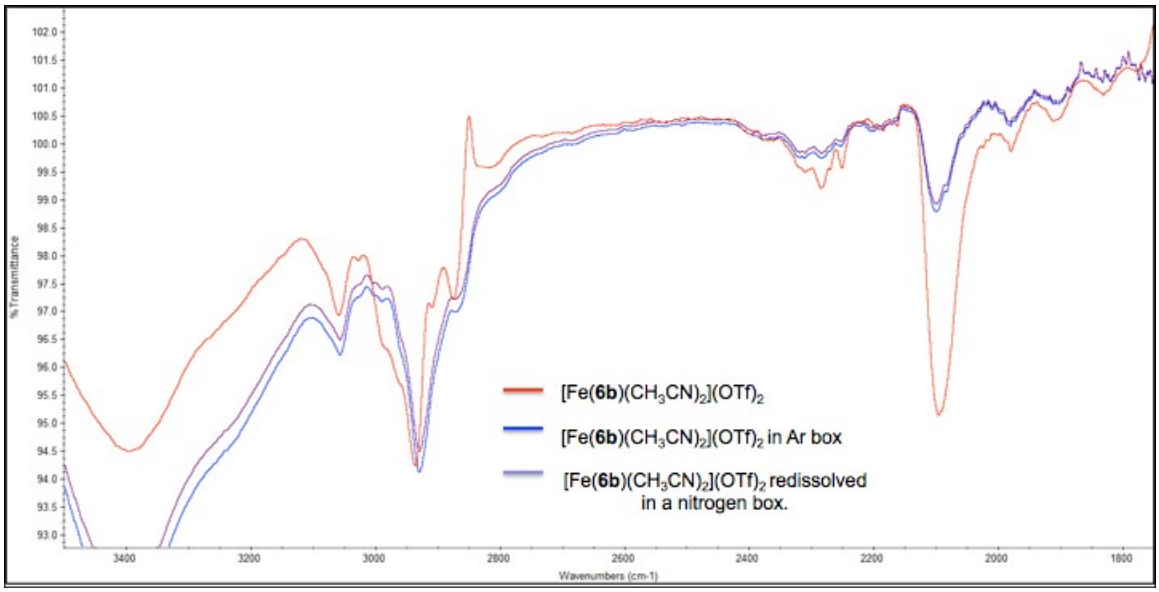

Figure S56. Overlay of [Fe(**21**)$(CH_3CN)_2$]$(OTf)_2$ prepared in an argon-filled glovebox vs. the same complex prepared in a nitrogen-filled glovebox.

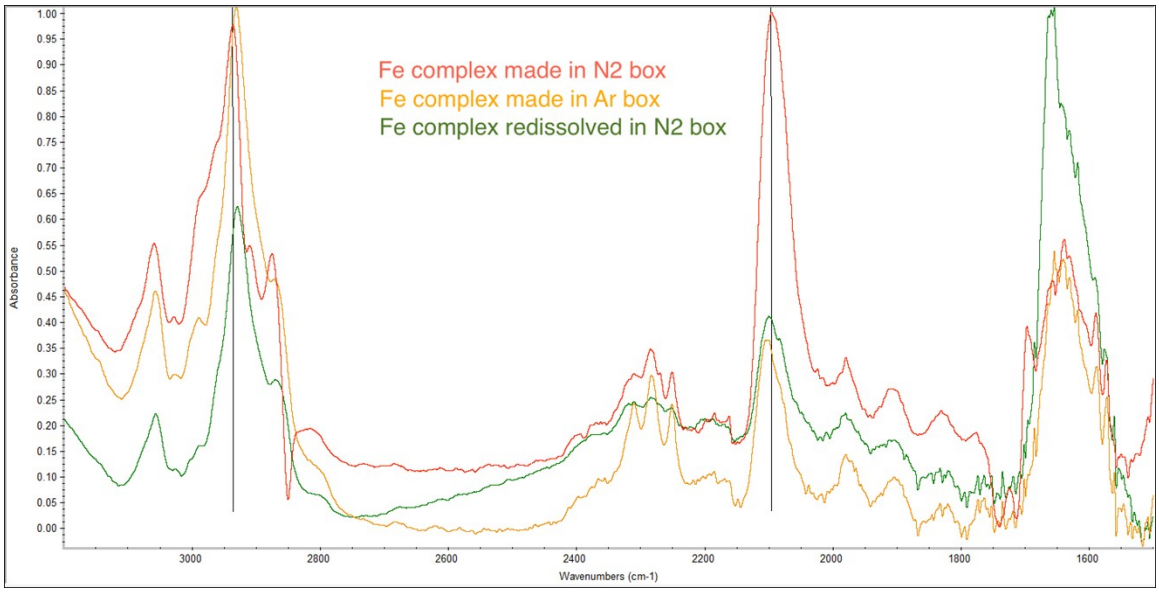

Figure S57. Overlay of [Fe(**21**)$(CH_3CN)_2$]$(OTf)_2$ prepared in an argon-filled glovebox vs. the same complex prepared in a nitrogen-filled glovebox (y-axis is absorbance).

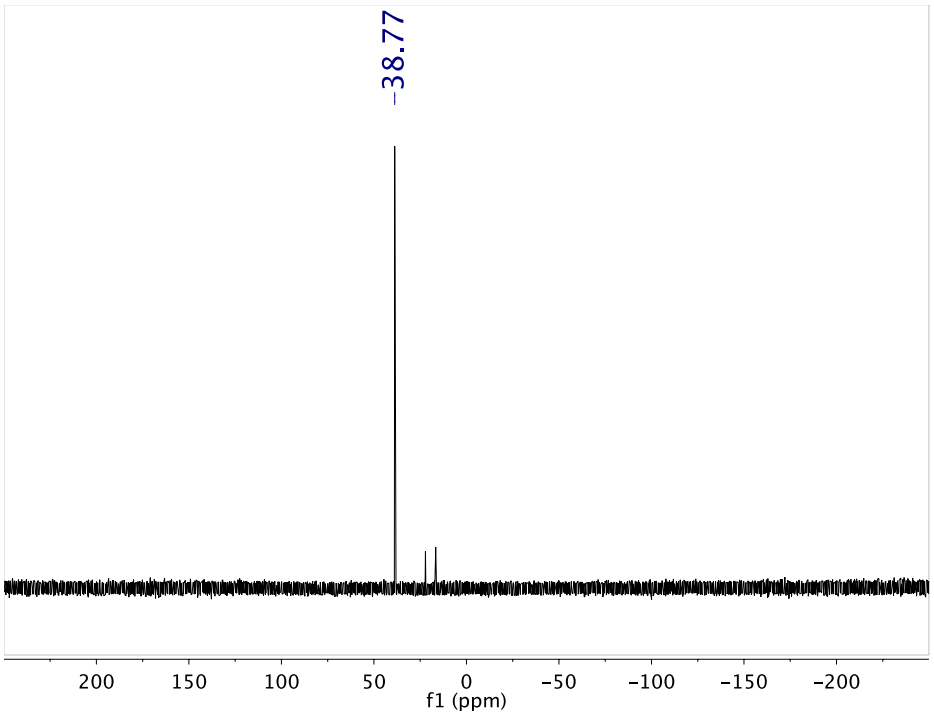

Figure S58. $^{31}P\{^{1}H\}$ NMR spectrum of isopropyl allyl(phenyl)phosphinate in $CDCl_3$.

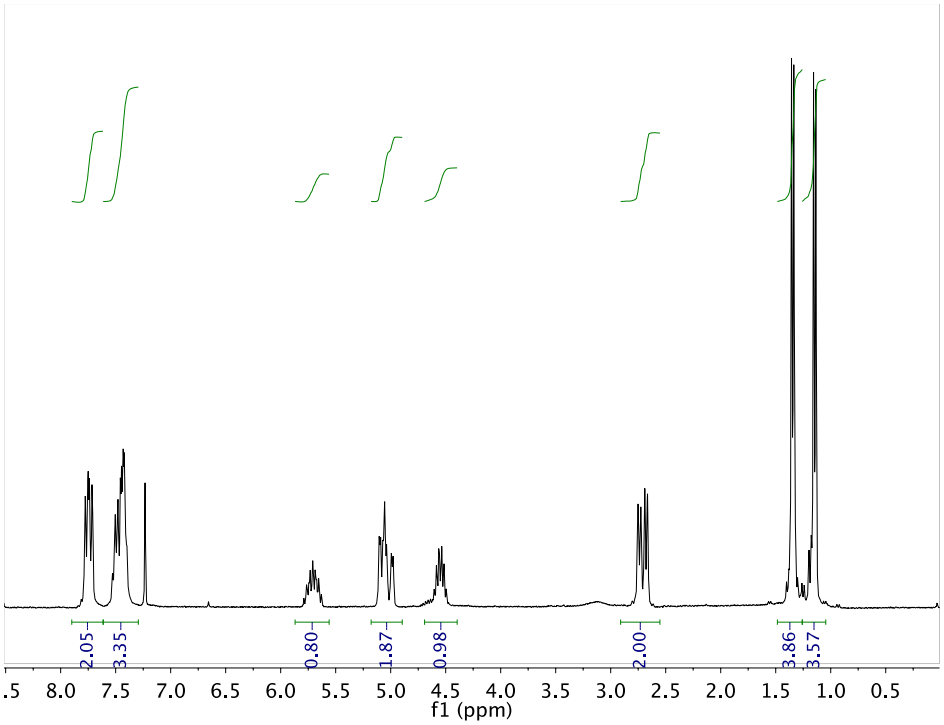

Figure S59. ^{1}H NMR spectrum of isopropyl allyl(phenyl)phosphinate in $CDCl_3$.

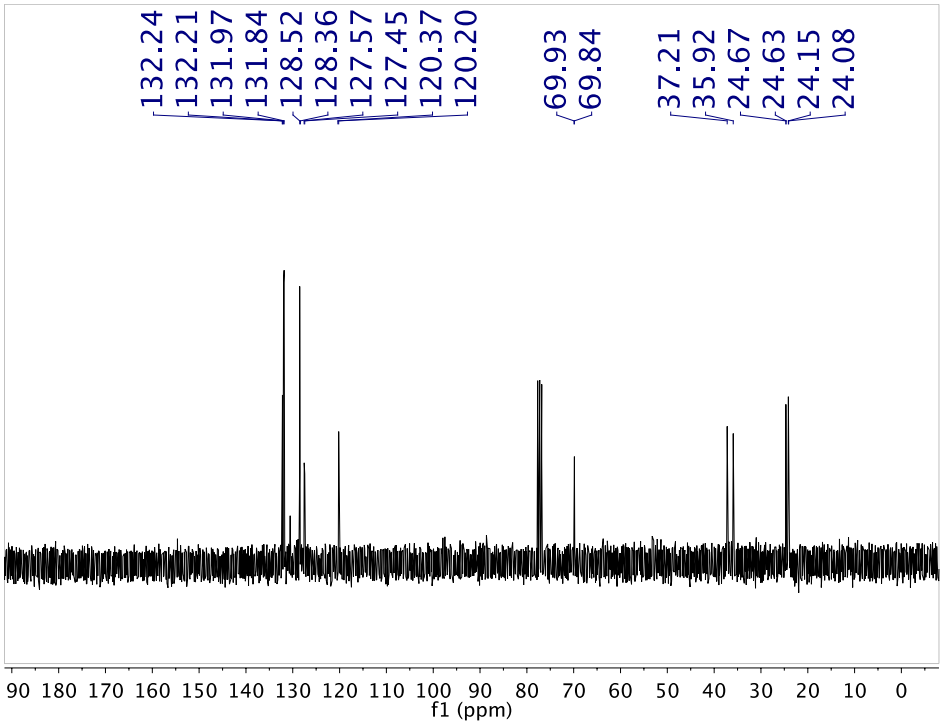

Figure S60. ^{13}C NMR spectrum of isopropyl allyl(phenyl)phosphinate in $CDCl_3$.

Table S2. Crystal data and structure refinement for **15**.

$C_{37}H_{44}CuF_3O_3P_4S$, M = 813.20, 0.21 x 0.12 x 0.06 mm, T = 150 K, Tetragonal, space group *I-4*, *a* = 13.207(4) Å, *b* = 13.207(4) Å, *c* = 10.681(4) Å, *V* = 1862.9(14) $Å^3$, *Z* = 2, D_c = 1.450 Mg/m^3, μ(Mo) = 0.865 mm^{-1}, *F*(000) = 844, $2\theta_{max}$ = 50.0°, 3231 reflections, 1536 independent reflections [R_{int} = 0.0696], R1 = 0.0822, wR2 = 0.2187 and GOF = 1.081 for 1536 reflections (94 parameters) with I>2σ(I), R1 = 0.1026, wR2 = 0.2337 and GOF = 1.081 for all reflections, max/min residual electron density +2.147/-0.489 $eÅ^{-3}$.

Table S3. Atomic coordinates (x 10^4) and equivalent isotropic displacement parameters ($Å^2$x 10^3) for mo_dtr26_0m_a. U(eq) is defined as one third of the trace of the orthogonalized U^{ij} tensor.

	x	y	z	U(eq)
Cu(1)	10000	10000	5000	38(1)
P(1)	8571(2)	9590(2)	4019(3)	38(1)
C(1)	8399(6)	8230(7)	3766(10)	46(3)
C(2)	8800(7)	7563(6)	4842(13)	52(3)
C(3)	9991(6)	7516(6)	5004(13)	46(2)
C(4)	8168(6)	10086(6)	2495(12)	48(3)
C(5)	7234(7)	9832(6)	2005(11)	46(3)
C(6)	6950(9)	10216(8)	874(14)	66(3)
C(7)	7570(8)	10877(8)	227(13)	58(3)
C(8)	8476(9)	11157(9)	698(12)	62(3)
C(9)	8794(7)	10772(6)	1874(11)	48(3)
O(1S)	10000	10000	690(30)	500(90)

Table S4. Bond lengths [Å] and angles [°] for mo_dtr26_0m_a.

Cu(1)-P(1)	2.225(2)
Cu(1)-P(1)#1	2.225(2)
Cu(1)-P(1)#2	2.225(2)
Cu(1)-P(1)#3	2.225(2)
P(1)-C(3)#2	1.827(10)
P(1)-C(1)	1.831(9)
P(1)-C(4)	1.834(12)
C(1)-C(2)	1.542(15)
C(1)-H(1A)	0.9900
C(1)-H(1B)	0.9900
C(2)-C(3)	1.584(13)
C(2)-H(2A)	0.9900
C(2)-H(2B)	0.9900
C(3)-P(1)#3	1.827(10)
C(3)-H(3A)	0.9900
C(3)-H(3B)	0.9900
C(4)-C(9)	1.394(13)
C(4)-C(5)	1.382(13)
C(5)-C(6)	1.363(16)
C(5)-H(5A)	0.9500
C(6)-C(7)	1.382(17)
C(6)-H(6A)	0.9500
C(7)-C(8)	1.349(17)
C(7)-H(7A)	0.9500
C(8)-C(9)	1.418(18)
C(8)-H(8A)	0.9500
C(9)-H(9A)	0.9500
O(1S)-O(1S)#4	1.48(7)
P(1)-Cu(1)-P(1)#1	123.82(14)
P(1)-Cu(1)-P(1)#2	102.81(6)
P(1)#1-Cu(1)-P(1)#2	102.81(6)
P(1)-Cu(1)-P(1)#3	102.81(6)
P(1)#1-Cu(1)-P(1)#3	102.81(6)

P(1)#2-Cu(1)-P(1)#3	123.82(14)
C(3)#2-P(1)-C(1)	106.7(4)
C(3)#2-P(1)-C(4)	100.2(5)
C(1)-P(1)-C(4)	100.6(5)
C(3)#2-P(1)-Cu(1)	107.7(4)
C(1)-P(1)-Cu(1)	114.4(3)
C(4)-P(1)-Cu(1)	125.3(3)
C(2)-C(1)-P(1)	114.1(7)
C(2)-C(1)-H(1A)	108.7
P(1)-C(1)-H(1A)	108.8
C(2)-C(1)-H(1B)	108.7
P(1)-C(1)-H(1B)	108.7
H(1A)-C(1)-H(1B)	107.6
C(1)-C(2)-C(3)	116.4(9)
C(1)-C(2)-H(2A)	108.2
C(3)-C(2)-H(2A)	108.2
C(1)-C(2)-H(2B)	108.1
C(3)-C(2)-H(2B)	108.3
H(2A)-C(2)-H(2B)	107.3
C(2)-C(3)-P(1)#3	109.5(6)
C(2)-C(3)-H(3A)	109.9
P(1)#3-C(3)-H(3A)	109.8
C(2)-C(3)-H(3B)	109.8
P(1)#3-C(3)-H(3B)	109.7
H(3A)-C(3)-H(3B)	108.2
C(9)-C(4)-C(5)	120.5(11)
C(9)-C(4)-P(1)	118.8(8)
C(5)-C(4)-P(1)	120.6(8)
C(6)-C(5)-C(4)	119.4(10)
C(6)-C(5)-H(5A)	120.3
C(4)-C(5)-H(5A)	120.4
C(5)-C(6)-C(7)	121.1(11)
C(5)-C(6)-H(6A)	119.5
C(7)-C(6)-H(6A)	119.4
C(8)-C(7)-C(6)	120.8(12)
C(8)-C(7)-H(7A)	119.6

C(6)-C(7)-H(7A)	119.6
C(7)-C(8)-C(9)	119.7(11)
C(7)-C(8)-H(8A)	120.2
C(9)-C(8)-H(8A)	120.1
C(4)-C(9)-C(8)	118.6(10)
C(4)-C(9)-H(9A)	120.7
C(8)-C(9)-H(9A)	120.7

Symmetry transformations used to generate equivalent atoms:

#1 -x+2,-y+2,z #2 y,-x+2,-z+1 #3 -y+2,x,-z+1

#4 y,-x+2,-z

Table S5. Anisotropic displacement parameters ($Å^2 x\ 10^3$)for mo_dtr26_0m_a. The anisotropic displacement factor exponent takes the form: $-2\pi^2[\ h^2a^{*2}U^{11} + ... + 2\ h\ k\ a^*\ b^*\ U^{12}\ ]$

	U^{11}	U^{22}	U^{33}	U^{23}	U^{13}	U^{12}
Cu(1)	25(1)	25(1)	63(2)	0	0	0
P(1)	28(1)	29(1)	58(2)	2(1)	0(1)	-5(1)
C(1)	29(4)	37(5)	71(8)	-3(4)	2(5)	0(3)
C(2)	47(5)	38(4)	72(8)	3(5)	-1(6)	-6(3)
C(3)	44(4)	31(4)	64(6)	0(6)	6(6)	9(3)
C(4)	26(4)	32(5)	84(8)	-8(5)	2(5)	3(3)
C(5)	40(5)	25(4)	73(8)	7(4)	0(5)	-2(3)
C(6)	66(7)	43(6)	88(9)	-9(6)	-9(7)	-6(5)
C(7)	57(6)	58(6)	60(8)	8(6)	3(6)	15(4)
C(8)	71(8)	53(6)	61(8)	-2(6)	9(6)	12(6)
C(9)	40(5)	27(4)	75(8)	2(5)	6(5)	-3(3)
O(1S)	900(200)	550(110)	25(19)	0	0	-400(140)

Table S6. Hydrogen coordinates (x 10^4) and isotropic displacement parameters ($Å^2$x 10^3) for mo_dtr26_0m_a.

	x	y	z	U(eq)
H(1A)	7668	8092	3651	55
H(1B)	8749	8036	2983	55
H(2A)	8548	6864	4711	63
H(2B)	8503	7812	5636	63
H(3A)	10321	7555	4174	56
H(3B)	10185	6867	5400	56
H(5A)	6793	9392	2452	55
H(6A)	6316	10027	525	79
H(7A)	7356	11138	-558	70
H(8A)	8898	11609	244	74
H(9A)	9420	10977	2230	57

Table S7. Torsion angles [°] for mo_dtr26_0m_a.

P(1)#1-Cu(1)-P(1)-C(3)#2	-148.2(3)
P(1)#2-Cu(1)-P(1)-C(3)#2	-33.0(3)
P(1)#3-Cu(1)-P(1)-C(3)#2	96.6(3)
P(1)#1-Cu(1)-P(1)-C(1)	93.4(4)
P(1)#2-Cu(1)-P(1)-C(1)	-151.4(4)
P(1)#3-Cu(1)-P(1)-C(1)	-21.9(4)
P(1)#1-Cu(1)-P(1)-C(4)	-31.2(4)
P(1)#2-Cu(1)-P(1)-C(4)	84.0(4)
P(1)#3-Cu(1)-P(1)-C(4)	-146.5(4)
C(3)#2-P(1)-C(1)-C(2)	-82.9(8)
C(4)-P(1)-C(1)-C(2)	173.0(7)
Cu(1)-P(1)-C(1)-C(2)	36.1(8)
P(1)-C(1)-C(2)-C(3)	-69.8(11)
C(1)-C(2)-C(3)-P(1)#3	86.3(11)
C(3)#2-P(1)-C(4)-C(9)	120.9(8)
C(1)-P(1)-C(4)-C(9)	-129.9(8)
Cu(1)-P(1)-C(4)-C(9)	0.4(9)
C(3)#2-P(1)-C(4)-C(5)	-55.4(8)
C(1)-P(1)-C(4)-C(5)	53.9(8)
Cu(1)-P(1)-C(4)-C(5)	-175.8(6)
C(9)-C(4)-C(5)-C(6)	3.4(14)
P(1)-C(4)-C(5)-C(6)	179.6(8)
C(4)-C(5)-C(6)-C(7)	-1.7(15)
C(5)-C(6)-C(7)-C(8)	0.2(17)
C(6)-C(7)-C(8)-C(9)	-0.3(17)
C(5)-C(4)-C(9)-C(8)	-3.4(14)
P(1)-C(4)-C(9)-C(8)	-179.7(7)
C(7)-C(8)-C(9)-C(4)	1.9(15)

Symmetry transformations used to generate equivalent atoms:

#1 -x+2,-y+2,z #2 y,-x+2,-z+1 #3 -y+2,x,-z+1

#4 y,-x+2,-z